Available online at www.sciencedirect.com
SCIENCE DIRECT
ELSEVIER
Coordination Chemistry Reviews 249 (2005) 2408–2436
COORDINATION CHEMISTRY REVIEWS
www.elsevier.com/locate/ccr

Review

Interplay between iron complexes, nitric oxide and sulfur ligands: Structure, (photo)reactivity and biological importance

Konrad Szaciłowski, Antonina Chmura, Zofia Stasicka *

Faculty of Chemistry, Jagiellonian University, Ingardena 3, 30-060 Kraków, Poland

Received 1 December 2004; accepted 17 March 2005
Available online 7 July 2005

Contents

Abstract

Nitric oxide is one of the most important signalling and regulatory molecule in all animal and plant organisms. Various iron complexes are involved in numerous steps of nitric oxide metabolism; most of these complexes contain diverse sulfur ligands. Nitric oxide is naturally generated from the amino acid arginine in the reaction catalyzed by an enzyme called nitric oxide synthase. The active centre of this enzyme contains an iron porphyrin complex with one thiolate axial ligand. Iron nitrosyls and nitrosothiols are the most relevant agents responsible for storage and transport of the NO and related compounds. Most of the target receptors of nitric oxide also contain iron centres and/or thiol groups. Nitrosothiols and metal nitrosylcomplexes belong to the most important external sources of nitric oxide (NO-donors). The most complex interactions are observed in ternary iron–sulfur–nitrosyl systems. Depending on the nature of the bond, the ternary iron–sulfur–nitrosyl species may be classified into two groups, (i) iron complexes with the *S*-nitrosothiol ligand, containing the {Fe–N(SR)O} moieties and (ii) RS–Fe–NO

* Corresponding author. Tel.: +48 12 633 53 92; fax: +48 12 633 53 92.
E-mail address: stasicka@chemia.uj.edu.pl (Z. Stasicka).

doi:10.1016/j.ccr.2005.03.021

compounds, where both NO and sulfurs are coordinated to the Fe-centre. Irrespective of the structure distinctness, the mutual interactions of all components are very strong due to considerable bond delocalization within both ternary systems. Some differences appear, however, in their sensitivity to the R nature.

Keywords: Nitric oxide; Iron complexes; Sulfur compounds; Fe–S–No systems; S–Fe–NO systems

1. Introduction

In recent years, the biochemical behaviour of nitric oxide is in the limelight of the world research [1–11]. It was also one of the principal interests of our research group. The interest was especially related to bioinorganic processes and included thermal [12–51] and photochemical [12–20,32–39,49–61] reactions of some nitrosyl complexes of transition metals, mainly iron. This research was aimed at the elucidation of the chemical mechanism of NO biosynthesis [62], the NO-donor metabolism [16,23,24,46–48,63] and improvement on therapeutic strategies of NO delivery [13,19,46,54,55,59,63,64]. Special attention was also paid to understanding the basic properties and reactivity patterns of nitrosyl complexes [12–48,51–58,60]. Recently, our research was expanded to *S*-nitrosothiols [16,24] and iron–sulfur clusters [52,65,66], whose biological activity is fairly well established and consists mainly in their cooperation with nitric oxide. Experimental work in model systems as well as in vitro experiments on cell cultures [52] and tissues [22] were supplemented with theoretical investigations [12,18,21,22,24,62,66–69].

Biological functions of nitric oxide and its redox forms are inherently related to the chemistry of thiol groups [70] and transition metal (mostly iron) centres [71] present in various biomolecules. All these three classes of compounds possess their distinct biochemical characteristics. Regulatory properties of nitric oxide are based on interactions with iron and sulfur moieties, redox properties of iron centres are in turn significantly modulated with protein-bound thiols and nitric oxide. They interact with each other and these mutual interactions may be responsible for most of the observed physiological and pathophysiological processes (Fig. 1); thus, the activity of binary and ternary iron–sulfur–nitrosyl systems is responsible for nitrosative regulation of metalloenzymes (I), nitric oxide storage and transport as *S*-nitrosothiols (II), redox tuning of iron–sulfur clusters and cytochrome P450-type enzymes (III), and regulation of immune system, NO biosynthesis storage (IV). The chemistry and photochemistry of *S*-nitrosothiols, iron nitrosyl complexes, iron–sulfur centres and iron–nitrosyl–sulfur complexes are useful and versatile tools that help us to understand the overwhelming diversity of biological processes.

This review article summarizes the ongoing research in the field of biologically relevant nitrosyl species in relation to various sulfur and iron compounds.

2. Physiological importance of nitric oxide ($NO^{\bullet}$) and its related forms (NO^{+}, NO^{-}, $ONOO^{-}$)

Nitric oxide, a simple stable radical, has emerged as one of the most fundamental molecules in biology and medicine [2–4,72]. Its wide spectrum of activity includes blood pressure control, smooth muscle relaxation, regulation of immune system, neurotransmission and countless other physiological effects [1,73–79]. Nitric oxide controls activity of different enzymes [16,70,71,74,80] via reversible coordination to iron (heme and non-heme) centres [71,80–85] and interaction with thiol groups [16,70].

Interactions of nitric oxide with biomolecules may be divided into three categories: protective, regulatory and deleterious (Fig. 2) [74,86]. Due to the relatively low oxidation state of the nitrogen atom, nitric oxide possesses significant antioxidative properties, whereas its free radical character allows it to rapidly and effectively scavenge oxidizing radicals. NO reacts with a series of highly deleterious oxidants, such as hydrogen peroxide, alkyl peroxides, superoxide and lipid-derived peroxides. The free radical reactivity of nitric oxide has some negative aspects too. It reacts easily with carbon-centred radicals in DNA resulting in formation of *C*-nitroso compounds. Such a modification of DNA strands prevents repair mechanisms and leads to mutations. This process is responsible for sensitization of cells to ionizing radiation and alkylating agents. The process has negative influence on living cells and is responsible for the cytotoxic effect of nitric oxide. It is, thus, used to support anticancer radiotherapy and chemotherapy [87,88].

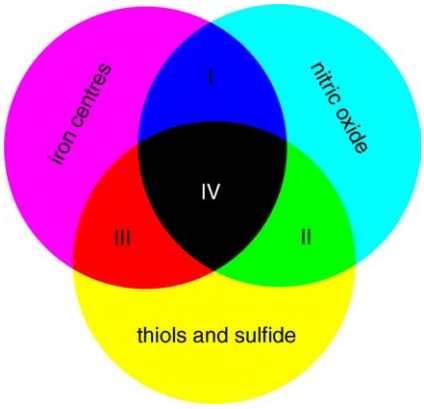

Fig. 1. Interplay between biologically important iron complexes, nitric oxide and sulfur ligands: iron nitrosyl complexes (I); *S*-nitrosothiols (II); iron–sulfur centers in proteins (III); iron–sulfur–nitrosyl complexes (IV).

Fig. 2. Multifaceted biological effects of nitric oxide [13,54,64,74,86].

Interaction of nitric oxide with metal centres of enzymes results in changes of their activity: activation or deactivation. Guanylate cyclase, hemoxygenase and T_fR protein are activated due to reaction with nitric oxide, while cytochrome oxidase, catalase, cytochrome P450, nitrile hydratase and proteases are inhibited. One of the most important enzymes utilizing nitric oxide is soluble guanylate cyclase [89,90]. This enzyme is responsible for cGMP synthesis, which is one of the most important NO-related signalling molecules. Reaction of nitric oxide with iron–sulfur centres may result in irreversible deactivation of their reactivity, one of the consequences of which is inhibition of mitochondrial respiration [71,73,86].

The extremely rich biological activity and chemical reactivity of nitric oxide suggest, that not only $NO^{\bullet}$, but also its reduced (NO^-) and oxidized (NO^+, $ONOO^-$) forms must significantly contribute to the nitric oxide biochemistry [91–97]. Redox reactions of nitric oxide with metalloproteins (Fig. 3), metal complexes and thiols (Fig. 4) may yield NO^- and NO^+ ions [8,16,96,97], whereas reaction with molecular oxygen yields $ONOO^-$ as a reactive intermediate [98]. Thiols react with the NO^+ sources yielding *S*-nitrosothiols, which in turn undergo homolytic S–N bond cleavage giving rise to $NO^{\bullet}$ and $RS^{\bullet}$ radicals (vide infra). *S*-nitrosothiols undergo nucleophilic attack on the nitrosyl moiety. When thiols or thiolate anions are the nucleophiles, the process results in the NO^+ transfer (transnitrosation) or formation of nitrosothiyl radicals, which may be the sources of NO^- or N_2O (vide infra) [16]. Metal ions (Cu, Fe, Co) can also induce oxidation or reduction of nitric oxide (Fig. 4).

Nitric oxide was reported to undergo reduction to nitroxyl anion at physiological pH in reaction with superoxide dismutase [99–101], reduced cytochrome *c* [102], ubiquinol [103] and nitric oxide synthase in the absence of tetrahydrobiopterin [104]. The NO^- anion in aqueous solution

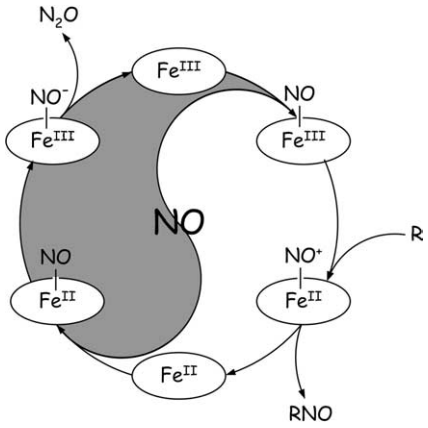

Fig. 3. The *yin-yang* of nitric oxide biochemistry. Porphyrin-catalyzed redox transformations of nitric oxide in biological systems. Adapted from [16].

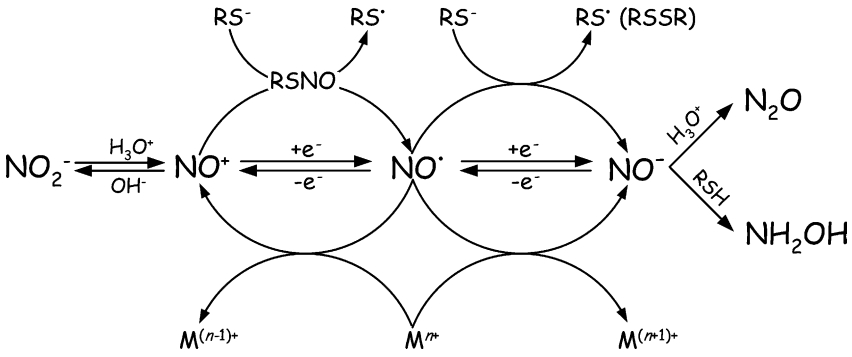

Fig. 4. Interconversion of different redox forms of nitric oxide in reactions with biologically relevant reducers and oxidants (M = Fe, Cu, Co). Adapted from [96].

is unstable and easily converted to N_2O [97,105,106]. Nitric oxide-binding to Fe^{II} hemoporphyrin proteins or oxidation of azide by lignin peroxidase also generates the NO^- ion [93]. The protonated form of NO^- (HNO) reacts with cysteine resulting in disulfide and hydroxylamine formation. The biological function of the nitroxyl anion is not fully characterized, but its role may involve redox reactions with glutathione and other intracellular thiols [107]. Recently, the protective role of nitroxide in heart diseases was reported [108]. Reaction of NO^- and HNO with molecular oxygen generates a series of reactive oxygen and nitrogen radical species showing high cytotoxicity. Another cytotoxic mechanism involves NO^--binding to iron–sulfur centres [93].

Oxidation of nitric oxide with molecular oxygen is a multistep, relatively slow reaction. In contrast, reaction between nitric oxide and superoxide anion is extremely fast and yields peroxynitrite anion, $ONOO^-$ [92,109]. Despite the high toxicity of peroxynitrite [110], nitric oxide is a protective agent against oxidative stress (vide supra) [74]. On the other hand, formation of higher concentrations of $ONOO^-$ may be responsible for nitric oxide cytotoxicity. Peroxynitrite induces a series of one-electron oxidation reactions, which eventually lead to lipid peroxidation. Two-electron oxidation induced by $ONOO^-$ affects aromatic structures in tocopherol and other biologically important antioxidants. Thiols generate thiyl radicals ($RS^\bullet$) and *S*-nitrosothiols; low molecular thiols and protein-bound thiols are considered as the principal $ONOO^-$ scavengers [95,111]. Metalloproteins and selenium proteins are also responsible for defence against peroxynitrite [95,111].

3. Physiological role of thiols, disulfides and related radicals

Sulfur occurs in proteins as a constituent of two amino acids: cysteine and methionine. The rich reactivity of these species allows an amazing variety of post-translational modifications of proteins and metal-free redox reactions. Unlike any other amino acid, cysteine participates in many redox transformations, which are the basis of activity of metal-free redox enzymes [112]. The redox activity of cysteine and methionine becomes especially distinct, when one considers the redox reactivity of a protein as a whole [113–116]. These amino acids endow proteins with powerful redox moieties on the side arms of the protein chain. Moreover, in contrast to most metal ions bound to proteins, which can exist only in two different oxidation states, sulfur in biological systems can be present in any oxidation state between −2 and +6 (Fig. 5).

The most abundant thiol in cellular medium is glutathione. This tripeptide is responsible for the maintenance of the global intracellular redox potential [117,118]. It also protects cell components against radical-induced damages and participates in many electron-transfer, atom-transfer and thiol/disulfide exchange reactions [119,120]. The latter processes are especially important for regulatory purposes (*S*-thionylation, *S*-glutathionylation), cell signalling and enzymatic functions.

Thiols react with various highly toxic O-, C-, S- and N-centred radicals yielding, via electron or hydrogen transfer reactions, thiyl radicals of lower toxicity than the original radicals (Fig. 6a) [95,112,119–121]. The thiyl radicals undergo, in turn, a series of reactions (Fig. 6b), but since in biological systems, the steady-state concentration of $RS^\bullet$ is very low, the dimerization is rather improbable. Thiyl radicals undergo addition to molecular oxygen, numerous free radicals and olefins yielding corresponding addition products (Fig. 6). They can also oxidize electron donors via electron abstraction or generate secondary radicals in hydrogen abstraction process. The fast addition of thiyl radicals to thiolate anions gives disulfide radical anions, $RSSR^{\bullet-}$ [24,121–131]. This anion radical is a strong reducing agent reacting with molecular oxygen, nitric oxide and metal ions and complexes (Fig. 6b) [24,121–131]. The S–S bond plays an important structural role in many proteins, because of the making and breaking of disulfide bonds are involved in control of the protein folding [112,125,132].

Involvement of nitric oxide and metal ions/complexes in thiol/thiyl radical reactivity pattern broadens significantly the range of possible biological responses (vide infra).

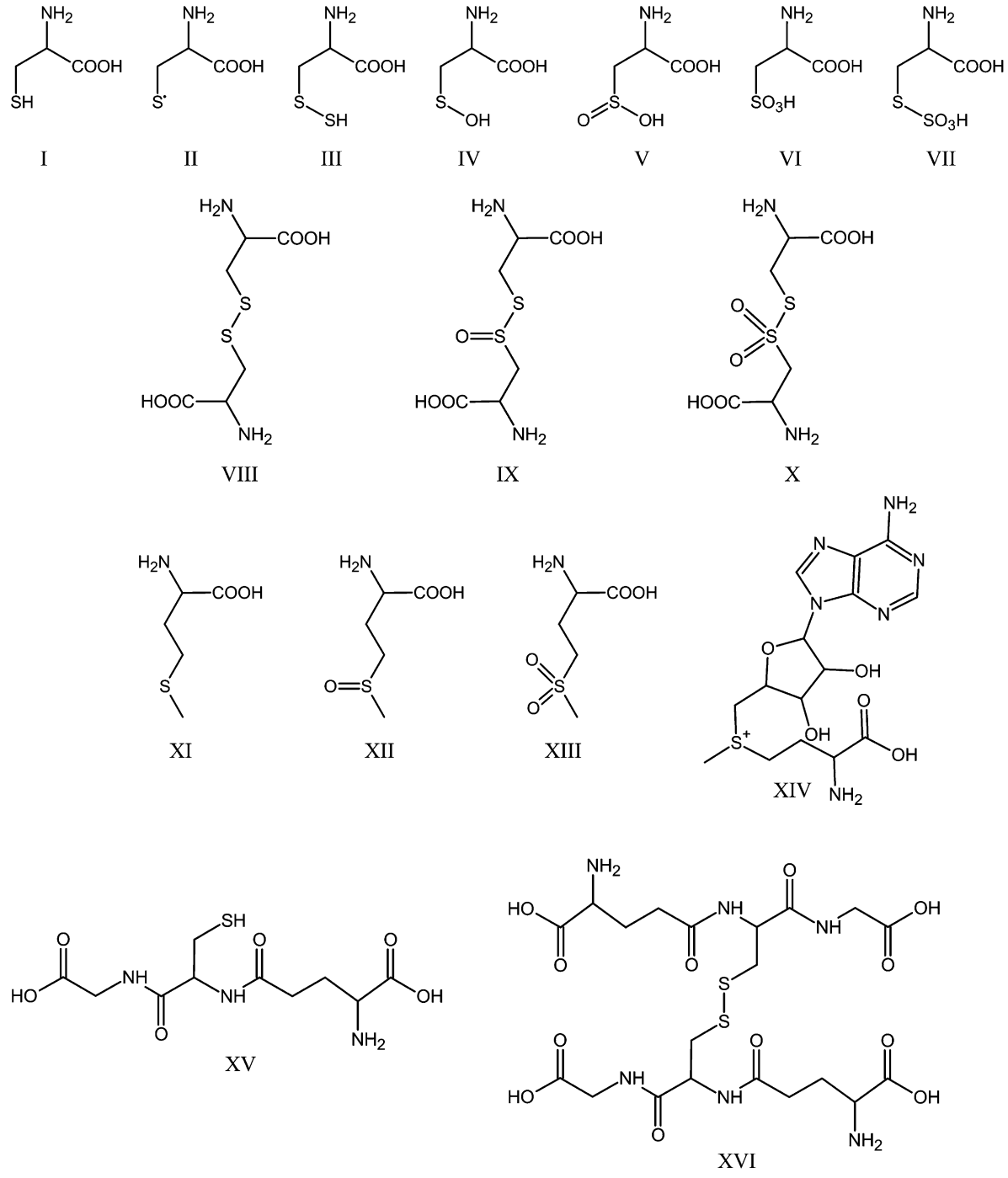

Fig. 5. Sulfur-containing amino acids and their redox modifications present in biological systems: cysteine (I); cysteinyl radical (II); *S*-sulfanyl cysteine (III); cysteine sulfenic acid (IV); cysteine sulfinic acid (V); cysteine sulfonic acid (VI); cysteine *S*-sulfate (VII); cystine (VIII); cystine *S*-monoxide (IX); cysteine *S,S*-dioxide (X); methionine (XI); methionine sulfoxide (XII); methionine sulfone (XIII), *S*-adenosyl methionine (XIV), glutathione (XV); glutathione disulfide (XVI).

4. Iron complexes in biological systems

Iron is the most abundant transition elements in the Solar System and Earth crust contains ∼6% of iron. The exceptional abundance of iron is justified by the very high stability of the Fe-nucleus, because of which iron is the final product of nucleosynthesis in stars. The abundance of iron in the Universe is reflected in its biological role. Iron is the most widespread transition metal in most living organisms and is involved in a multitude of bioprocesses. Versatility of its compounds is a result of ready redox Fe^{II}/Fe^{III} transformations and rich coordination chemistry involving

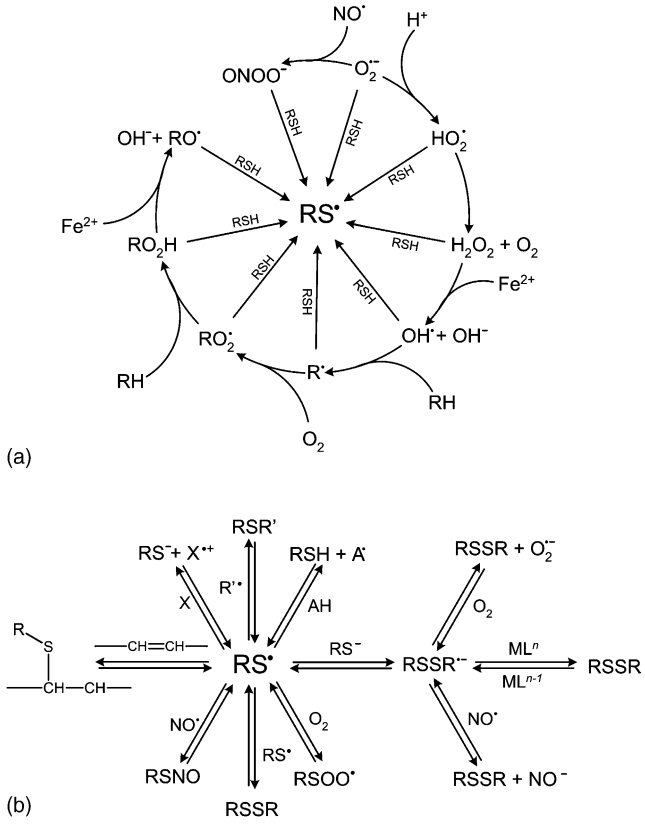

Fig. 6. Formation (a) and decay (b) pathways of thiyl radicals in biological systems. Adapted from [95,112,119–121,130].

various ligands present in biological systems: amino acids, thiols, phenols and porphyrins [133,134]. A human body of average weight contains approximately 4.8 g of iron [135], most of which is bound in hemoglobin, the rest is mainly in the form of ferritin, myoglobin, cytochromes and other proteins.

Iron ions are very frequently present in the active sites of enzymes and other important proteins [136]. Iron complexes in biological systems are involved in the following functions: (i) stabilization of tertiary and quaternary protein structure; (ii) iron uptake and storage; (iii) electron-transfer reactions; (iv) dioxygen-binding and activation (O_2 transport and storage, O_2 reduction and O atom insertion); (v) substrate activation by the electrophilic behaviour of iron [134]. To fulfil all these duties, a large variety of iron coordination species are engaged which can be divided into four principal classes: mononuclear iron proteins, dinuclear iron carboxylates, iron–sulfur clusters and iron porphyrins (Fig. 7) [137,138]. The most abundant iron complexes in biological systems are the porphyrin complexes and Fe–S clusters. Other biologically important complexes include iron carboxylates and complexes with O- and N-donor amino acid residues. All these metalloenzymes can be regarded as classical coordination compounds, where protein counterpart is a complex supramolecular ligand that keeps all the donor atoms in desired spatial arrangement, shields the reactive centre from undesired reagents and provides access channels and binding sites for proper substrates [134]. In many cases, the protein ligand modulates the redox properties of the iron centre, this is especially evident in the case of iron–sulfur proteins [139,140] and P450-type enzymes [141,142].

Tetrapyrrolic pigments were developed early during evolutionary processes and still are very common in biological systems [143,144]. The most common are iron porphyrin complexes. There are nine different iron-complexing porphyrin ligands, which are relevant in biological systems (Fig. 8) [137,138]. They differ in the number and structure of terminal substituents and double bonds within the macrocyclic system. These differences allow for various anchorages within the protein (covalent via side chains, coordination through axial ligand or hydrophobic interactions) and versatile biological functions. The principal functions of the heme proteins include oxygen transport, storage and activation, electron-transfer and sensing processes [81,85,144–147]. Depending on the heme structure and axial coordination, heme proteins play various functions. Chlorocruoroheme and heme *b* are most common in globins, which are responsible for oxygen transport and storage [148–150]. Heme *b* is also found in cytochromes P450, chloroperoxidases, bacterioferritins, nitrophorins, soluble guanylate cyclases and peroxidases [151,152]. In all these proteins, Fe in heme is axially coordinated with histidine, except for cytochromes P450 and chloroperoxidases utilizing cysteine (vide infra) and bacterioferritins-containing methionine ligands. Heme *d*, with axially coordinated phenolate is an active centre of catalases, i.e. enzymes that catalyze reaction of peroxide decomposition. Catalases induce decomposition of hydrogen peroxide yielding molecular oxygen and water in the disproportionation reaction [153]. Hemes *a* and *o* (with axial histidine) are found in cytochrome *c* oxidases, iron–copper enzymes involved in dioxygen reduction [154]. Cytochromes *c* can be defined as electron-transfer proteins having one or several heme *c* groups, bound to the protein by one or, more commonly two, thioether bonds involving sulfhydryl groups of the cysteine residues. A histidine residue always provides the fifth ligand to iron in heme. Cytochrome *c* has a wide range of properties and is engaged in a large number of different redox processes [155]. Heme d_1 is found in cytochrome cd_1 nitrite reductase, a bifunctional enzyme that catalyzes both the one-electron reduction of nitrite to nitric oxide and two-electron reduction of oxygen to water. These reactions are key respiratory processes in denitrifying bacteria. The enzyme contains one covalently bound heme *c* and a noncovalently bound heme d_1, which appears to be the site of nitrite and oxygen reduction, whereas heme *c* accepts the electrons from donors, such as azurin, pseudoazurin and cytochrome c_{551} [156,157]. The unusual heme P460 is found in hydroxylamine oxidoreductase, the enzyme which catalyzes the four electron oxidation of hydroxylamine to nitrite. It is abundant in a nitrifying chemoautotrophic bacterium *Nitrosomonas*

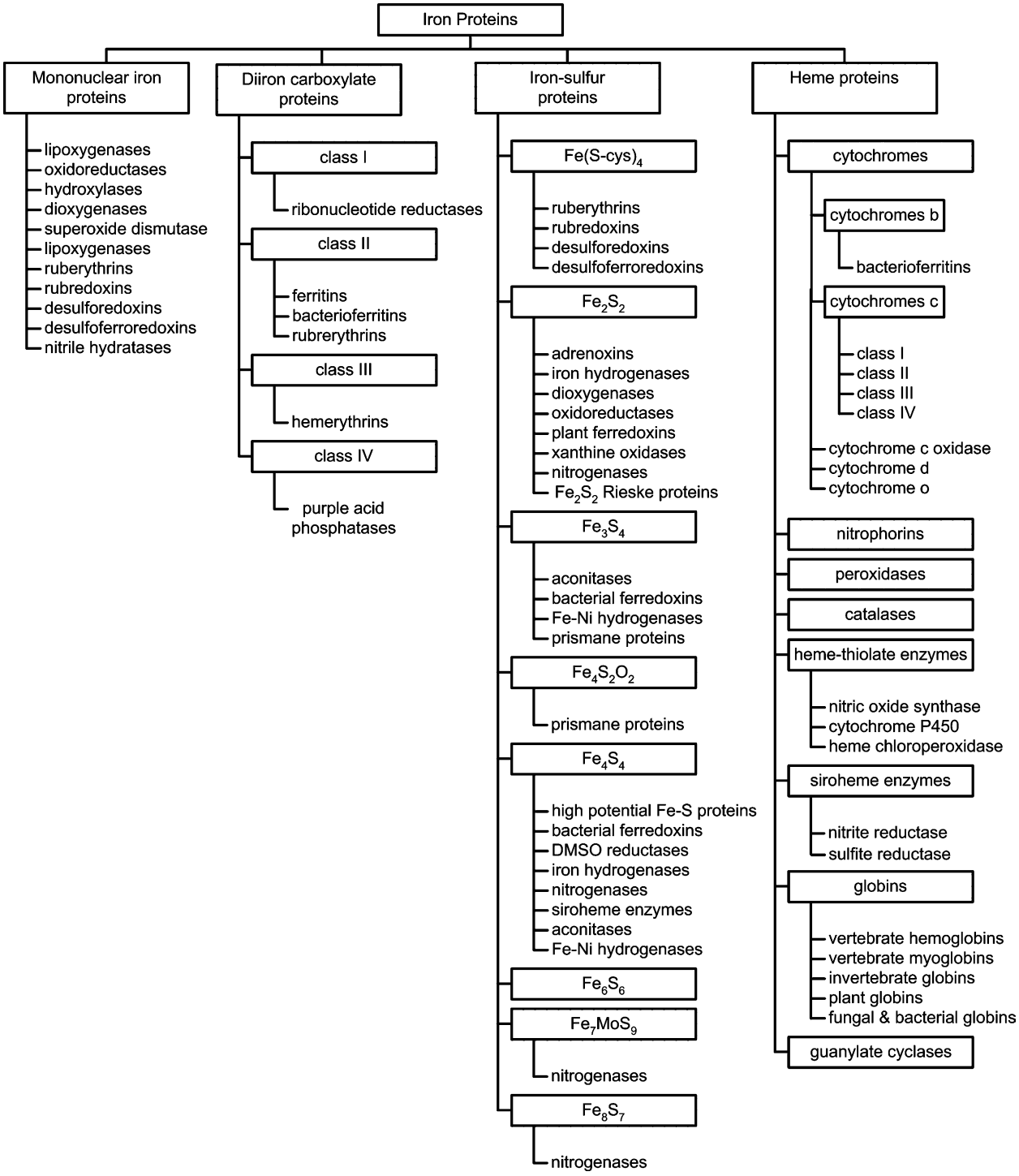

Fig. 7. Classification of the most important iron proteins [137,138].

europaea and is a key enzyme in the respiratory chain [158].

The most complex iron centre is present in siroheme proteins: nitrite reductase and sulfite reductase. It contains Fe_4S_4 cubane moiety coupled with the siroheme iron-complex via cysteine bridge. These enzymes are efficient catalysts in nitrite and sulfite reduction (vide infra) [159–162].

5. Binary systems

5.1. Thiols and nitric oxide: chemistry of S-nitrosothiols

S-Nitrosothiols (other common name thionitrites) are thiol derivatives formed via substitution of proton in the –SH group with nitrosonium cation. Their physiological role is very

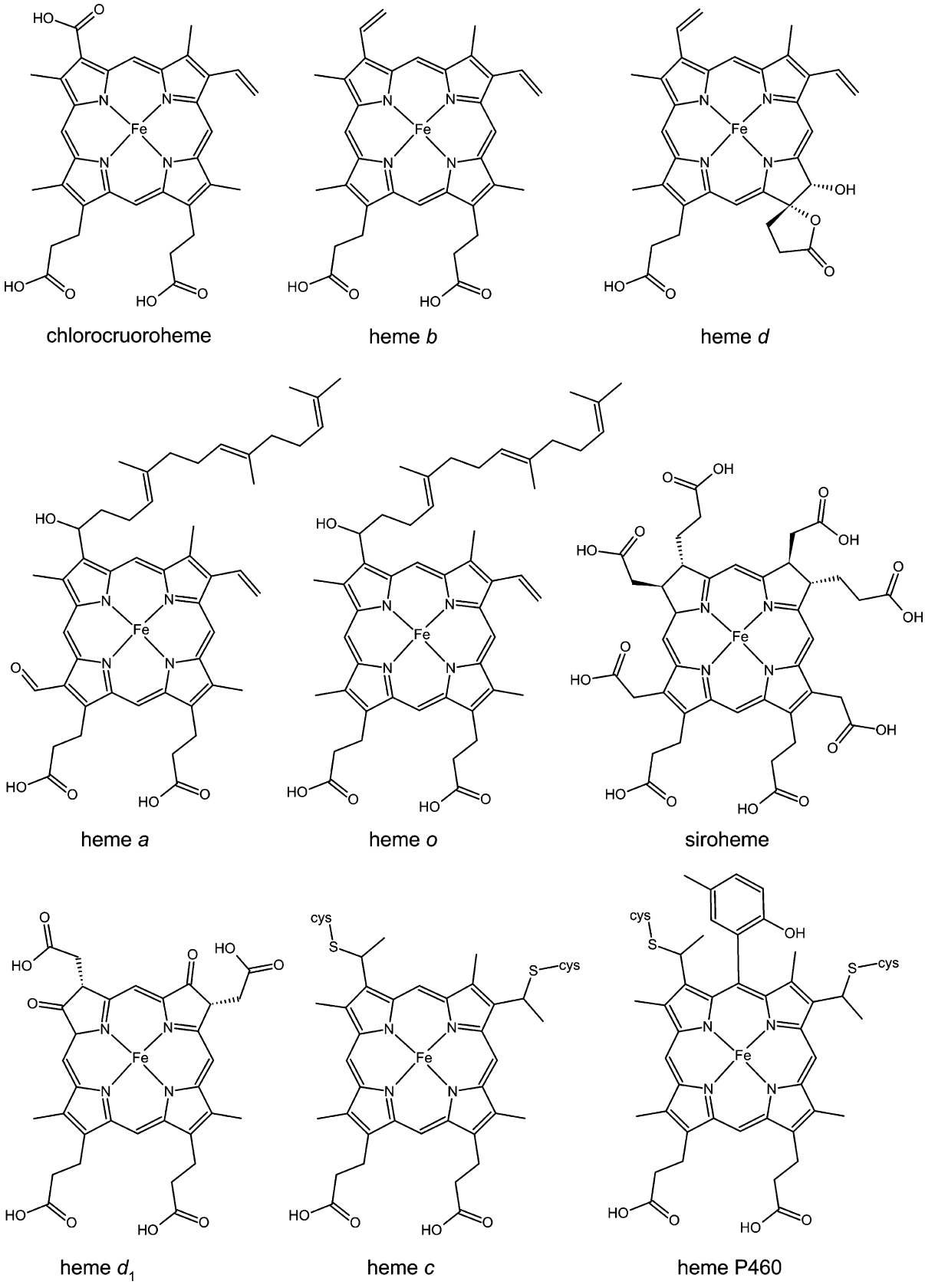

Fig. 8. Molecular structure of various heme moieties found in iron proteins [137,138].

important; they are the principal stores of nitric oxide; they participate in NO redox changes (cf. Fig. 4), are the source of thiyl radicals and are involved in some regulatory processes.

Nitrosothiols are usually formed in reactions between thiols and various nitrosation agents, including nitric oxide in the presence of electron acceptors, nitrosonium salts, nitrous acid and inorganic nitrites, metal nitrosyl complexes and many others [16].

Due to their instability very few *S*-nitrosothiols have been characterized crystallographically [163–165]. The C–S–N–O framework is almost planar and adopts an *anti* conformation. The C–S bond lengths in the compounds (182–186 pm) are similar to the C–S distance in methionine (181 pm) and aliphatic disulphides (185–186 pm) and correspond to the single C–S bond. The S–N distances (176–186 pm) indicate a single bond and can be compared with that in sulphaminic acid (177 pm). The N–O bond in RSNO (117–120 pm) should be referred to as a double bond as it is significantly shorter than in NO^- (126 pm) but longer than in NO^+ (106 pm) and even than in NO (115 pm). The S–N–O angles (114.0–116.7°) are in harmony with the double N–O bond conception. The structural data are, thus, consistent with the resonance structure (I) presented in Fig. 9. A more detailed comparison of the S–N and N–O distances shows, however, a decrease in the S–N distance and increase in the N–O bond length in tertiary, and especially, *N*-acylated tertiary *S*-nitrosothiols, which is consistent with the increased contribution of the structure (II). There is also a spectroscopic evidence for a significant contribution of form (II) in substituted *S*-nitrosothiols [16].

S-Nitrosothiols are usually thermally unstable and undergo spontaneous decomposition via homolytic splitting of the S–N bond according to the Eqs. (1) and (2):

$$RSNO \rightleftarrows RS^{\bullet} + NO^{\bullet} \quad (1)$$

$$2RS^{\bullet} \rightarrow RSSR \quad (2)$$

The thiyl radical generated in the first, reversible step is very reactive and can combine to corresponding disulfide (2) or undergo addition to various reactants, among others to dioxygen (3) or thiolate anion (4) (cf. Fig. 6).

$$RS^{\bullet} + O_2 \rightarrow RSOO^{\bullet} \quad (3)$$

$$RS^{\bullet} + RS^- \rightleftarrows RSSR^{\bullet -} \quad (4)$$

The RSNO thermal stability is controlled thus by strength of the S–N bond. Recently, DFT calculations showed that the S–N bond is very weak, its dissociation energy amounts 28 kcal mol^{-1} [166]. In reality, it is affected by the alkyl chain structure. In general, *S*-nitrosothiols are the more stable the higher contribution of the resonance structure (II) (Fig. 9), which in turn is effected, e.g. by the electron releasing substituents. Apart from electronic effects, steric hindrance affecting the efficiency of thiyl radical recombination (2) also has its contribution to the stability of *S*-nitrosothiols [167].

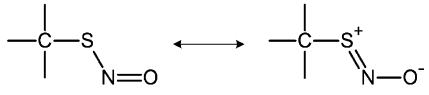

I II

Fig. 9. Resonance structures of *S*-nitrosothiols.

S-Nitrosothiol irradiation within both its absorption bands leads to fast photochemical decomposition. As in the thermal reaction, the primary products are thiyl radicals and nitric oxide [16].

The biological importance of *S*-nitrosothiols is mainly based on their ability to react with numerous nucleophiles, including thiols and amines. The reaction may consist in simple nitrosyl transfer (so called *transnitrosation*, Eqs. (5) and (6), thiyl radical addition or may involve complex redox transformations, both under aerobic and anaerobic conditions (Fig. 10) [16,168–170]. The interactions of *S*-nitrosothiols with metal centres leads to formation of nitrosyl complexes, while interactions with organic nucleophiles results in the formation of various nitrosation products. Other possible pathways include glutathionylation and tyrosine nitration [16,168–170].

$$RSNO + R'SH \rightleftarrows RS(R'S)NOH \quad (5)$$

$$RS(R'S)NOH \rightleftarrows RS'NO + RSH \quad (6)$$

The 1,2 addition of thiol to *S*-nitrosothiol yields an intermediate $(RS)_2NOH$ (or RS(R′S)NOH), which may decompose either heterolytically yielding transnitrosation product ((5) and (6)) [171,172] or participate in the Tannenbaum reaction (7) [173,174] yielding ammonia as a final product.

$$(RS)_2NOH + 3RSH \rightarrow RSOH + 2RSSR + NH_3 \quad (7)$$

The other pathway that can initiate the Tannenbaum reaction is a nucleophilic attack of a thiolate anion on the *S*-nitrosothiol entity (8).

$$RSNO + RS^- \rightleftarrows (RS)_2NO^- \xrightarrow{H_3O^+} (RS)_2NOH \quad (8)$$

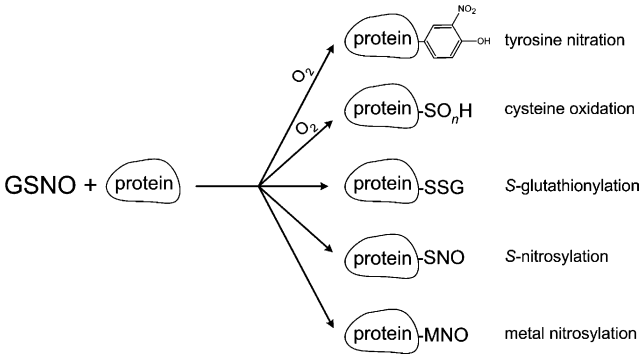

Fig. 10. Various modes of post-translational reversible and irreversible modification of proteins induced by *S*-nitrosoglutathione (and possibly other *S*-nitrosothiols). The same processes are also involved in cellular signalling, enzymatic regulation, inflammatory processes and others [168–170].

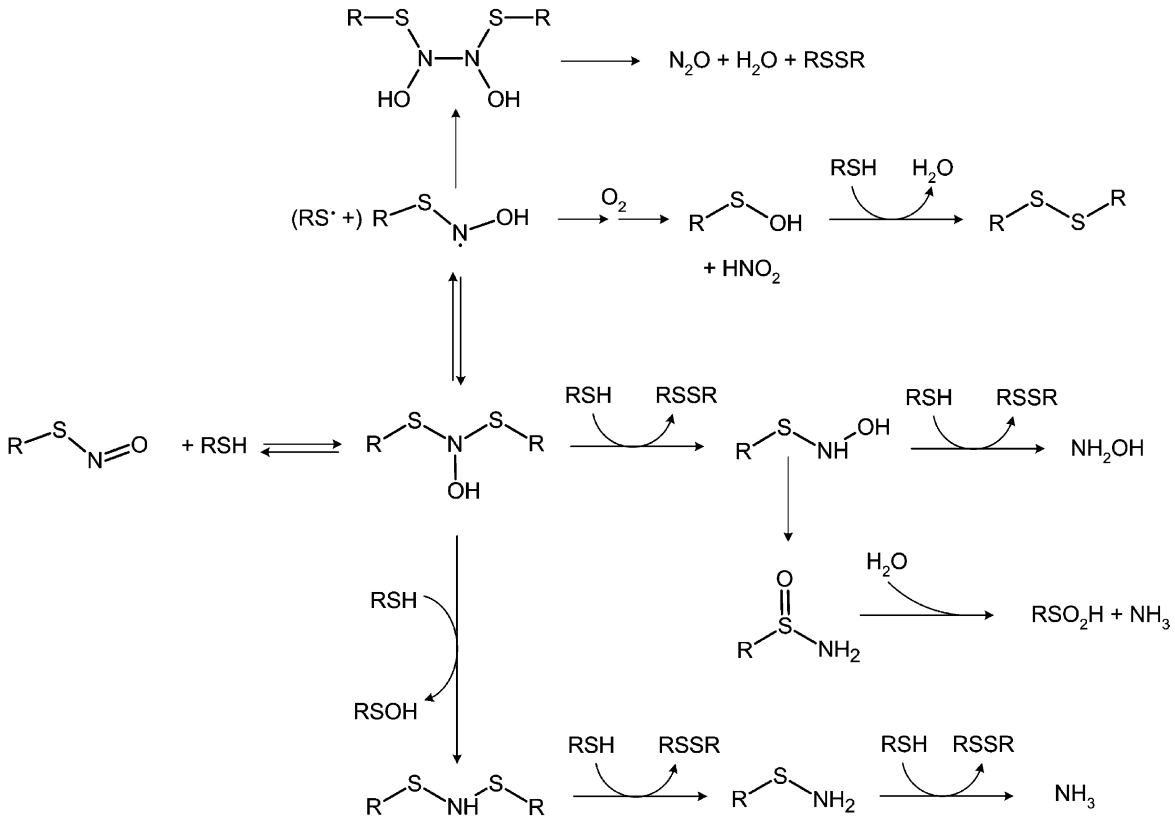

Fig. 11. General scheme of reactivity in the *S*-nitrosothiol–thiol system ([16,173] and references therein).

The overall scheme of these reactions is shown in Fig. 11. This possibility was recently analyzed theoretically [24]. The propensity of the RSNO to undergo a nucleophilic attack of a thiolate anion is confirmed by the character of the frontier orbitals of the reactants. The HOMO orbital of the thiolate anion is localized mainly (90%) on the sulfur atom, while the LUMO orbital of the nitrosothiol is distributed between oxygen (15%), nitrogen (50%) and sulfur (30%) atoms [24], as shown in Fig. 12.

These transformations of *S*-nitrosothiols, especially the transnitrosation processes, belong to the very important cellular signalling channels. While phosphorylation (perhaps the most common signalling process) is enzyme-driven, the transnitrosation relies only on chemical properties of the reactants [168]. Many transcription factors like NF-κB, hypoxia-inducible factors (HIF), zinc finger transcription factors, metalloproteins and others are activated via *S*-nitrosation of cysteine residues. They control many important processes, like angiogenesis, wound healing, DNA repair and synthesis and cellular respiration [168].

5.2. Iron–sulfur complexes

Iron–sulfur complexes and clusters are important prosthetic groups for many metalloenzymes (Fig. 13) [134,136–138,175–177]. They constitute the most ancient, ubiquitous, structurally and functionally diverse class of enzymes. Their primary function is mediation of one-electron redox processes, substrate-binding and maintenance of protein structure. The iron–sulfur proteins may be regarded as the interface between inorganic and biological world [161,186,187]. Some hypotheses assume that iron–sulfur compounds were the first catalytic systems on Earth and probably were of prime importance to biogenesis, especially near high-temperature volcanic vents, as iron and sulfur compounds are still the source of energy for chemoautotrophic organisms living under these extreme conditions [187,188]. Enzymes containing Fe–S cores usually catalyze reactions involving components of the Earth's primordial atmosphere, as N_2, CO and H_2 [189].

Transition metal ions tend to form cluster complexes with chalcogenide anions [190–200]. Iron and sulfur are unique elements in the sense that no other two elements can generate so large a diversity of cluster structures [199]. This is the consequence of two stable oxidation states of iron ions, strong Fe–S bonds of significant covalent character and bridging multiplicities two to six for sulfide [199]. Moreover, numerous structures are stable in several oxidation states, and therefore, these clusters serve as electron reservoirs in biological systems [201].

Apart from simple monomeric complexes like $[Fe(SR)_4]^-$, numerous oligomeric species containing 2–18 iron ions are formed [193,199,200,202–205]. Structures containing infinite polymeric chains are also reported

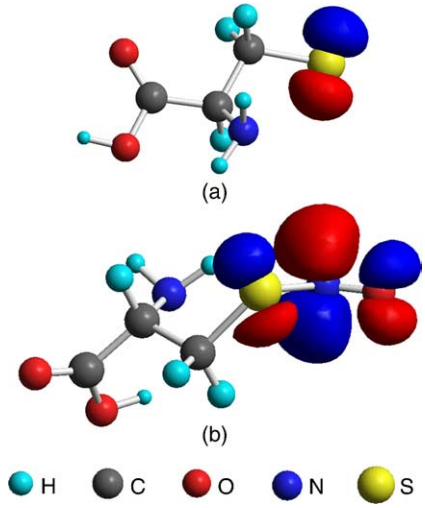

Fig. 12. Plot of molecular orbitals: HOMO of cysteinate anion (a) and LUMO of *S*-nitrosocysteine (b) [24].

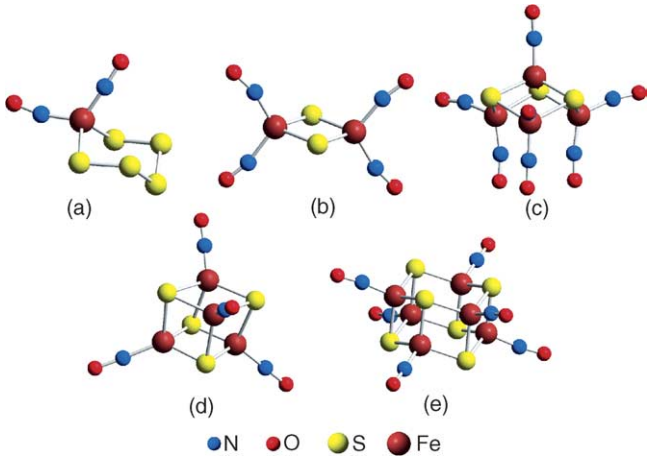

Fig. 14. X-ray structures of the most important iron–sulfur–nitrosyl clusters: (a) $[FeS_5(NO)_2]^-$; (b) $[Fe_2(\mu_2\text{–}S)_2(NO)_4]^{2-}$; (c) $[Fe_4(\mu_3\text{–}S)_3(NO)_7]^-$; (d) $[Fe_4(\mu_3\text{–}S)_4(NO)_4]$; (e) $[Fe_6(\mu_3\text{–}S)_6(NO)_6]^{2-}$. Based on crystallographic data from Refs. [210–214].

[206]. Despite the structural diversity of iron–sulfur clusters all of them are built from very few simple building blocks. The principal constitutional unit for the majority of the Fe–S clusters is the $[Fe_2S_2]$ rhomb [191,207,208]. Edge sharing, Fe-vertex sharing and S-vertex sharing lead to various complex structures. Also, the cubic core $[Fe_4S_4]$ may be treated as a building block in some more complex structures of higher nuclearity (cf. Fig. 13f and g) [159,209]. In natural systems the protein-bound Fe–S units are usually coordinated by cysteine ligands, in some cases histidine and proline ligands are also found. Synthetic analogues of Fe–S units may contain a large variety of terminal ligands, including thiolates, phosphines, amines, cyclopentadienes, carbonyls and nitrosyls [193]. Regardless of the cluster structure, its charge and nature of the terminal ligand, the Fe–S bond lengths, Fe–S–Fe and S–Fe–S bond angles are very similar. The Fe–S distance falls within 2.15–2.35 Å, the acute Fe–S–Fe angle within 74–76° and the obtuse S–Fe–S angle within 103–115° [193,207].

Iron–sulfur clusters constitute the integral parts of several natural structures occurring in a large family of biologically relevant metalloproteins. The [Fe–S] units form there the active sites of enzymes, which play a crucial role in living organism processes, such as electron trans-

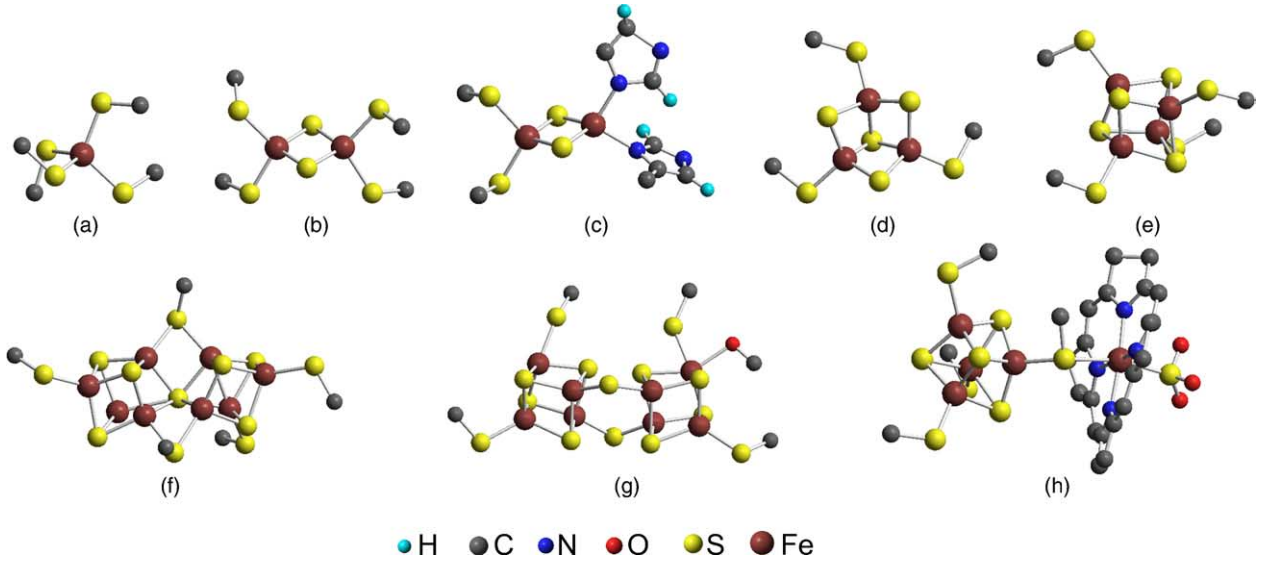

Fig. 13. Crystallographic structures of the most important iron–sulfur centres in proteins: (a) monomeric complex in *Clostridium pasteurianum* rubredoxin [178]; (b) dimeric centre in ferrodoxin from *Spinacia oleracea* [179]; (c) dimeric centre of Rieske protein from *Thermus thermophilus* [180]; (d) trimeric centre of ferredoxin from *Bacillus schlegelii* [181]; (e) cubane cluster of nitrogenase reductase from *Azotobacter vinelandii* [182]; (f) nitrogenase octameric cluster from *Azotobacter vinelandii* [183]; (g) nitrogenase octameric cluster from *Clostridium pasteurianum* [184]; (h) active centre of sulphite reductase from *Escherichia coli* [185].

fer in photosynthesis and cellular respiration, nitrogen fixation and many other catalytic reactions; they can also operate as biosensors of oxidants and iron ions. There are four principal iron–sulfur structures observed in biological systems: $[Fe(SR)_4]^n$, $[Fe_2S_2(SR)_2]^n$, $[Fe_3S_4(SR)_2]^n$ and $[Fe_4S_4(SR)_4]^n$ [134] (Fig. 13). Centres containing up to eight iron ions are supposed to be derived from smaller clusters [137] via sulfide or thiolate bridging (vide supra). The structures of these iron centres are almost preserved in all iron–sulfur proteins, while their redox potentials vary from −600 to +500 mV, a range larger than for any other simple redox cofactor. At the same time, all the bond lengths and angles within the FeS moiety are almost unchanged. The same fundamental Fe–S structures are also maintained in the Fe–S–NO systems (Fig. 14, vide infra). This illustrates the great versatility of the iron–sulfur core, where its interactions with thiolate ligands effectively tune the redox properties of the cluster [139,140]. Similar phenomena were observed in the case of substituted iron dithiocarbamates [215,216].

Iron–sulfur interactions are also very important for the modulation of the activity of cytochrome P450 enzymes. The active site of these proteins contains heme *b* centre with axially coordinated cysteine. The principal function of these enzymes is the oxidative transformation of exogeneous and endogeneous molecules. The principal reactions catalyzed by P450 enzymes include: hydroxylation of saturated carbon-hydrogen bonds, epoxidation of double bonds, oxidation of heteroatoms, oxidation of aromatic systems and other species utilizing molecular oxygen as an oxidant. The first step of the reaction includes coordination of molecular oxygen to the reduced heme centre followed by heterolytic scission of the O–O bond and insertion of oxygen atom into the organic substrate [217–222]. The heterolysis of the O–O bond is assisted by synergistic effects of distal and proximal environment of the heme centre. These interactions are usually called the "pull" and "push" effects, respectively [223]. A detailed theoretical study shows, that axial thiolate coordination facilitates the O–O bond cleavage due to the field effect of the negatively charged ligand and also tunes/modifies the redox properties of the Fe^{II}/Fe^{III} couple [223]. Moreover, the good σ-donor properties of the thiolate ligand allow for the efficient mixing of resonance forms of the ferryl centre (cf. Fig. 22), which results in sensitivity of the active centre towards medium polarity and non-covalent interactions. The versatility of the P450-type enzymes is, thus, the result of interactions between iron centre, porphyrin ring and thiolate ligand.

5.3. Iron nitrosyls in biological systems

Nitric oxide reacts with many transition metal compounds, but the chemistry of iron complexes is undoubtedly the richest one [8,19,30,80,224,225]. In biological systems, the interactions of NO with iron centres is currently believed to be the most important NO signalling mechanism. Reversible binding of nitric oxide by heme iron in guanylate cyclase activates the enzyme and induces synthesis of cGMP, one of the most important messenger molecules [82,226,227]. Other enzymes, like nitrile hydratase, were found to be reversibly deactivated by nitric oxide-binding [83,84,228–231]. The photodissociation of nitric oxide is a key mechanism of nitrile hydratase regulation. Blood flow and hence oxygen delivery is also controlled by interaction of nitric oxide with hemoglobin, both with heme centre and cysteine [232–238]. Interactions between iron centres and nitric oxide may be also involved in NO transport and storage [239–244]. Various model systems have been developed to study these interactions and numerous review papers deal with this complex subject in detail [8,19,30,80,231,245–248]. The structure and reactivity of iron nitrosyl complexes depends both on co-ligands and oxidation state of the iron centre. Iron porphyrins are involved in redox transformations of nitric oxide (vide infra, cf. also Figs. 3 and 4). Details of the biological aspects of nitric oxide interactions with iron complexes are described in this volume by Macyk et al. [249].

6. Ternary systems: chemistry of iron–sulfur–nitrosyl species with the FeN(SR)O framework

The interplay between iron complexes, sulfur-containing ligands and NO is involved in a multitude of biological processes like nitric oxide biosynthesis, different regulatory processes and nitrosyl-induced carcinogenesis. The versatile and complex chemistry and photochemistry of various abiological systems containing iron complexes with sulfur and nitrosyl ligands reflects well the complexity of these unique systems.

In a majority of these compounds, sulfur and nitric oxide interactions are indirect, through the iron centre, which enables the versatility of the whole (RS–Fe–NO) moiety, whereas in some other cases, sulfur and nitric oxide interact directly, forming the more complex, *S*-nitrosothiol ligand N(SR)O coordinated to the iron centre, {Fe–N(SR)O}. In the latter case, the ligand effect is somewhat different than in the former, but its influence on the Fe-centre can be easy modified by change of the R-substituent [23,24].

A good example showing the complexity of interactions in the iron–nitrosyl–thiol system, Fe–N(SR)O, is the thermal and photochemical reactivity of the pentacyanonitrosylferrate(2−) complex with aliphatic thiols. This apparently simple system, first described in 1915 [250], shows very rich and complex reactivity.

6.1. Thermal reactivity

One of the most studied nitrosyl complexes is pentacyanonitrosylferrate(2−), commonly known as nitroprusside. In alkaline solution, nitroprusside reacts with thiolates yielding a dark red nitrosothiol complex of the type $[Fe(CN)_5N(SR)O]^{3-}$ [23]:

$$[Fe(CN)_5NO]^{2-} + RS^- \rightleftarrows [Fe(CN)_5N(SR)O]^{3-} \quad (9)$$

The same complex can be obtained in reaction between thermally stable *S*-nitrosothiols and pentacyanoferrates(II) with a labile ligand [23]:

$$[Fe(CN)_5NH_3]^{3-} + RSNO \rightarrow [Fe(CN)_5N(SR)O]^{3-} + NH_3 \quad (10)$$

$$[Fe(CN)_5H_2O]^{3-} + RSNO \rightarrow [Fe(CN)_5N(SR)O]^{3-} + H_2O \quad (11)$$

In most cases, the product of the reaction is thermally unstable and undergoes an intramolecular redox reaction yielding $[Fe(CN)_5NO]^{3-}$ and disulfide as the main products [23,24]. The absorption spectrum of the nitrosothiol complex is very different from the spectra of the parent compounds (Table 1). The principal absorption band, localized at 522–528 nm, has dominant MLCT character with some MC contribution. The energy of this transition is slightly affected by the thiolate structure (522 nm for glutathione, 528 nm for 2,3-dimercaptopropanol) and by the nature of cation present in solution (in the case of mercaptosuccinate 526 nm for Li^+ to 530 nm for *N*,*N*′-dimethyl-4,4′-bipyridinum) [23].

The equilibrium (9) is extremely sensitive to different stimuli, like pH, cation type and concentration, temperature, pressure and light [15]. Increasing pH shifts the equilibrium to the right. The pH-dependence profile is almost identical with the titration curve of the specific thiol. The effect of ionic environment is more complex. Increasing ionic strength at constant cation concentration shifts the equilibrium (9) to the left, while increasing cation concentration to the right. Increasing ionic strength at constant cation concentration can be achieved only by exchanging monovalent anions with divalent ones. Divalent anions can compete effectively with nitroprusside in ion pair formation. Moreover, increasing ionic strength decreases mean activity coefficients according to Debye–Hückel Eq. [15]. The role of cation consists primarily in reduction of electrostatic repulsion between anionic reagents, thus, shifting the equilibrium (9) to the right. Moreover, interaction of cations with the $[Fe(CN)_5N(SR)O]^{3-}$ complex stabilizes the weak N–S bond changing charge distribution in the complex. This in turn increases the $[Fe(CN)_5N(SR)O]^{3-}$ stability in the presence of cations forming stable ion pairs (Table 2) [15,23].

Table 1
Spectroscopic characteristics of *S*-nitrosomercaptosuccinate, nitroprusside and the $[Fe(CN)_5N(SR)O]^{3-}$ complex

λ_{max} (nm)	ε_{max} ($M^{-1}\,cm^{-1}$)	Transition	References
S-Nitrosomercaptosuccinate			
230	5100	$\pi \rightarrow \pi^*$	[16]
336	840	$n_O \rightarrow \pi^*$	[16]
546	16	$n_N \rightarrow \pi^*$	[16]
$[Fe(CN)_5NO]^{2-}$			
200	24000	$MLCT_{Fe \rightarrow CN}$	[251]
237	700	$\sigma_{CN} \rightarrow \pi^*_{NO}$	[12]
		MC	[252,253]
264	900	$MLCT_{Fe \rightarrow NO}$	[12]
		MC	[252,253]
330	50	MC	[253,254]
393	25	MC + LC	[12]
		$MLCT_{Fe \rightarrow NO}$	[252–254]
497	8	MC	[12]
		$MLCT_{Fe \rightarrow NO}$	[252–254]
$[Fe(CN)_5N(SR)O]^{3-}$, RS^- = mercaptosuccinate			
318	1320	MLCT + LC	[23]
526	6000	MLCT	[23]

The thermal stability of the $[Fe(CN)_5N(SR)O]^{3-}$ complex also depends strongly on the thiolate structure and the lifetime of these complexes varies from seconds to days [23,24]. Carboxylic groups increase, while amino groups decrease the thermal stability of the thiolate adduct. This can easily be associated with the electron density shift within the thiolate molecule due to the inductive effect of the substituent. Electronegative carboxylates depleting electron density of sulfur atoms inhibit electron transfer to the iron centre and thus stabilize the complex. The opposite effect is exerted by amino groups. Esterification of –COOH and acylation of $–NH_2$ groups reduces their effect, while methylation of the amino groups enhances destabilization of the $[Fe(CN)_5N(SR)O]^{3-}$ complex. Beside the electronic density shift, the thiol structure can enhance the complex stability by formation of a six-membered ring, as is illustrated in Fig. 15. The lifetime of the $[Fe(CN)_5N(SR)O]^{3-}$ complex decreases in the series (Table 3) [23]:

N-acetylcysteine > cysteine > ethyl cysteinate;
mercaptoethanol > cysteamine > *N*,*N*-dimethylcysteamine;
mercaptosuccinate > 2-mercaptopropionate > 3-mercaptopropionate.

The thermal decomposition of the $[Fe(CN)_5N(SR)O]^{3-}$ species is a complex process. A detailed kinetic study showed that the presence of oxygen and excess of any of the reagents has an enormous influence on the reaction mechanism [24]. The principal product, the $[Fe(CN)_5NO]^{3-}$ complex, is formed in homolytic splitting of the N–S bond (Fig. 16).

In excess of nitroprusside, the reaction (12) proceeds according to first-order kinetics and follows the rate law for the system with pre-equilibrium (13).

$$[Fe(CN)_5N(SR)O]^{3-} \rightleftarrows [Fe(CN)_5NO]^{3-} + RS^{\bullet} \quad (12)$$

$$k_{obs}^{NP} = \frac{K_9 k_{12}[NP]}{1 + K_9[NP]} + k_{-12} \quad (13)$$

The rate of innersphere decomposition of the $[Fe(CN)_5N(SR)O]^{3-}$ complex ($k_{12} + k_{-12}$) depends on the thiolate structure, which is consistent with previously observed inductive effect [23,24]. The formation of a six-membered ring by *N*-acylated thiols [16] results in strengthening of the S–N bond at the expense of weakening of the N–O bond (Fig. 15). This effect may contribute

Table 2
Thermodynamic functions for the formation of the $[Fe(CN)_5N(SR)O]^{3-}$ (RS = mercaptosuccinate) complex in presence of different cations (0.2 M aqueous solutions) at pH 10 [15]

Cation[a]	Radius (pm[b])	ΔH (kJ mol^{-1})	ΔS (J mol^{-1} K^{-1})	ΔV (cm^3 mol^{-1})
Li^+	307	−31.1	−89.5	−14.9
Na^+	292	−24.1	−62.7	−14.2
K^+	279	−29.7	−77.0	−13.45
Cs^+	277	−45.9	−125.3	−11.3
Me_4N^+	298	−72.5	−226.2	−15.5
Et_4N^+	320	−43.4	−136.6	−20.4
Pr_4N^+	362	−21.8	−71.0	−13.0
Bu_4N^+	396	−12.1	−38.6	−7.9

[a] Introduced as chloride or bromide.
[b] Mean ionic radii existing in solution (hydrated or naked), calculated according to the data from Ref. [255].

also to the increased stability (the lowest $k_{12} + k_{-12}$ values) in the case of thiols with a substituted amino group (i.e. *N*-acetylcysteine and glutathione). Moreover, the strength of the S–N bond in the $[Fe(CN)_5N(SR)O]^{3-}$ complex correlates well with the strength of the S–H bond in thiols. The higher pK_a value of the thiol dissociation, the less probable is spontaneous decomposition of the $[Fe(CN)_5N(SR)O]^{(n+2)-}$ complex. In this case, oxygen has no effect on the kinetics of the reaction studied.

In excess thiolate, the decomposition of the $[Fe(CN)_5N(SR)O]^{3-}$ complex proceeds much faster (up to two orders of magnitude) and the kinetic traces indicate some autocatalytic behaviour. The main process responsible for this effect is the reaction between thiolate anions (present in large excess) and the thiyl radicals (generated in reaction 12) [24,121–131].

$$RS^\bullet + RS^- \rightleftarrows RSSR^{\bullet -} \quad (14)$$

Disulfide radical anions are very strong electron donors and nucleophiles, so they can efficiently react with both complexes present in the system (i.e. the $[Fe(CN)_5NO]^{2-}$ and $[Fe(CN)_5N(SR)O]^{3-}$ complexes) (Eqs. (15)–(17), Fig. 16).

$$[Fe(CN)_5N(SR)O]^{3-} + RSSR^{\bullet -} \rightleftarrows [Fe(CN)_5N(SR)_2O]^{4-} + RS^\bullet \quad (15)$$

$$[Fe(CN)_5N(SR)_2O]^{4-} \rightleftarrows [Fe(CN)_5NO]^{3-} + RSSR^{\bullet -} \quad (16)$$

$$[Fe(CN)_5NO]^{2-} + RSSR^{\bullet -} \rightleftarrows [Fe(CN)_5NO]^{3-} + RSSR \quad (17)$$

Reactions (15) and (16) provide chain propagation, while reaction (17) terminates the autocatalytic chain. At very high thiolate excess, however, the latter is rather insignificant, because equilibrium (9) is strongly shifted towards the $[Fe(CN)_5N(SR)O]^{3-}$ complex. Thiyl radical coupling and heterolytic decomposition of the $[Fe(CN)_5N(SR)_2O]^{4-}$ intermediate yielding $[Fe(CN)_5N(SR)O]^{3-}$ and thiolate may also contribute to the chain termination. The most efficient

Table 3
Influence of thiol structure on the $[Fe(CN)_5N(SR)O]^{3-}$ complex stability [23]

Thiol	$\tau^a_{1/2}$ (s)	Thiol	$\tau_{1/2}$ (s[a])	Thiol	$\tau_{1/2}$ (s[a])
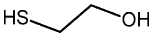	80	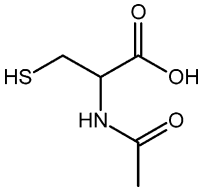	450	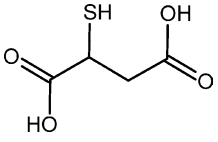	>130000
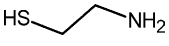	25	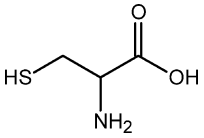	140	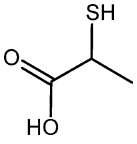	6500
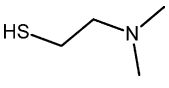	20	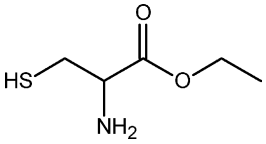	70	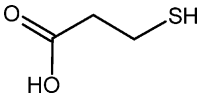	500

[a] Half-life time.

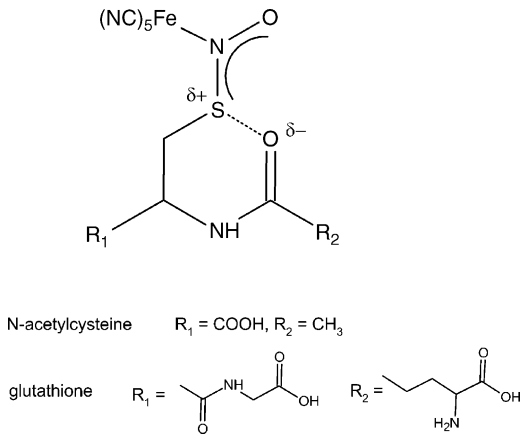

Fig. 15. Model of intramolecular stabilization of the N—S bond due to formation of the six-membered rings in the $[Fe(CN)_5N(SR)O]^{3-}$ complexes with the *N*-acylated thiols (*N*-acetylcysteine and glutathione) [16,24].

chain terminator is, however, molecular oxygen. In the presence of oxygen, the $[Fe(CN)_5N(SR)O]^{3-}$ decomposition proceeds only slowly with concomitant oxygen consumption. When all oxygen is consumed, reaction becomes faster and proceeds with the rate characteristic for anaerobic system (Fig. 17) [23,24]. This behaviour can be easily explained in terms of disulfide radical anion; it reacts with oxygen (cf. Fig. 6) much faster than with the complexes (Eqs. (15) and (16)), and therefore, the autocatalytic chain is inhibited. Rapid removal of oxygen and oxygen-derived radicals results in increasing concentration of $RSSR^{\bullet-}$ and as a consequence, decomposition of the $[Fe(CN)_5N(SR)O]^{3-}$ complex is accelerated.

Considering the influence of the sulfur subunit on the nitrosylpentacyanoferrate(II) properties, its main impact consists in changing the electron distribution within the complex, which results not only in crucial changes in the spectroscopic properties (cf. Table 1), but also in assisting $[Fe(CN)_5NO]^{3-}$ formation by switching the sp hybridization of N-atom within the nitrosyl ligand into the sp^2 one.

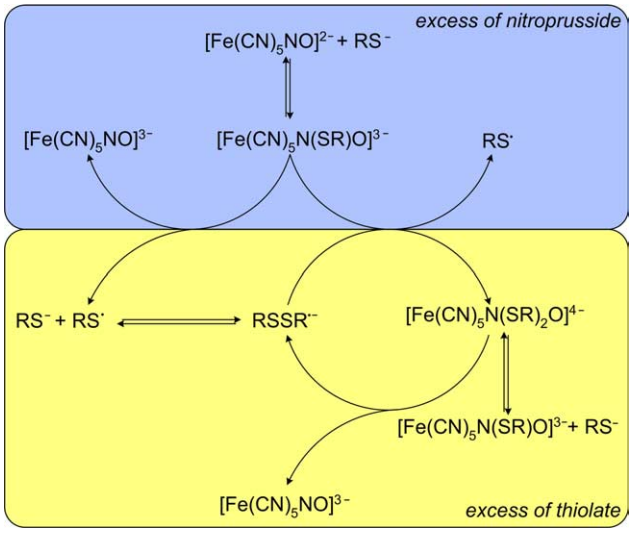

Fig. 16. Simplified mechanism of decomposition of the $[Fe(CN)_5N(SR)O]^{3-}$ complex in the presence of excess of nitroprusside (upper panel) and thiolate (lower panel). Reactions involving thiyl radicals and disulfide radical anions are omitted for the clarity (cf. Fig. 6) [24].

6.2. Photochemistry

The photochemistry of the nitroprusside ion is well-documented. Exposure to high-energy radiation ($\lambda \leq 313$ nm) induces photoreduction (18):

$$[Fe(CN)5NO]^{2-} + solv \xrightarrow{h\nu} [Fe(CN)_5NO]^{3-} + solv^{\bullet+} \quad (18)$$

whereas irradiation with light of lower energy ($313 < \lambda < 500$ nm) causes photooxidation–substitution reaction (19).

$$[Fe(CN)_5NO]^{2-} + OH^- \xrightarrow{h\nu} [Fe(CN)_5OH]^{3-} + NO^{\bullet} \quad (19)$$

The principal products are nitric oxide and the $[Fe(CN)_5OH]^{3-}$ complex ($\lambda_{max} = 392$ nm, $\varepsilon = 1800\ M^{-1}\ cm^{-1}$), but due to the photoreactivity of $[Fe(CN)_5OH]^{3-}$ and/or of its protonated form, prolonged irradiation leads to free cyanide, dicyan and other products [33,35,40,53,57,58].

The photochemistry of the $[Fe(CN)_5N(SR)O]^{3-}$ complex is more complicated due to secondary reactions, but photooxidation processes follow a similar pattern. Two principal pathways involve photodissociation and photooxidation–substitution modes. The MLCT excitation populates antibonding orbital of RSNO-ligand, which results in charge separation and yields the $[Fe^{III}(CN)_5\{N(SR)O^{\bullet-}\}]^{3-}$ intermediate. Population of the antibonding orbital weakens the S–N bond and causes its heterolytic splitting.

$$[Fe^{II}(CN)_5N(SR)O]^{3-} \xrightarrow{h\nu} [Fe^{III}(CN)_5\{N(SR)O^{\bullet-}\}]^{3-} \quad (20)$$

$$[Fe^{III}(CN)_5\{N(SR)O^{\bullet-}\}]^{3-} \rightarrow [Fe^{II}(CN)_5NO]^{2-} + RS^- \quad (21)$$

This reaction (21) leads to the same products as the reverse of reaction (9). Inner sphere photoinduced electron transfer may also induce other type of reactivity. The $[Fe^{III}(CN)_5\{N(SR)O^{\bullet-}\}]^{3-}$ intermediate formally contains the coordinated *S*-nitrosothiyl radical. It is only weakly bonded with the Fe-centre and readily dissociates (Eq. (22)). The vacant site is then occupied by the thiolate ligand present in solution (Eq. (23)).

$$[Fe^{III}(CN)_5\{N(SR)O^{\bullet-}\}]^{3-} \rightarrow [Fe(CN)_5]^{2-} + RSNO^{\bullet-} \quad (22)$$

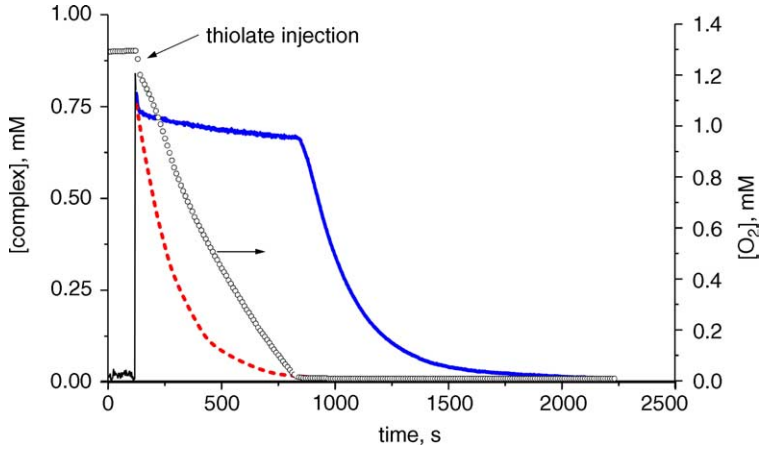

Fig. 17. Kinetic traces of the $[Fe(CN)_5N(SR)O]^{3-}$ complex decomposition observed in the system containing nitroprusside (1 mM) and 2-mercaptopropionate (50 mM). Dashed curve was recorded under anaerobic conditions, while the solid one was recorded for a solution saturated with oxygen. Circles indicate oxygen concentration.

$$[Fe(CN)_5]^{2-} + RS^- \rightarrow [Fe(CN)_5SR]^{3-} \quad (23)$$

The resulting $[Fe(CN)_5SR]^{3-}$ complex is characterized by a strong LMCT absorption band at 700 nm ($\varepsilon = 2800\ M^{-1}\ cm^{-1}$). The $RSNO^{\bullet-}$ radical undergoes numerous reactions yielding RSNO and $Fe(SR)_2(NO)_2]^-$ [15,55–57]. Its reaction with nitroprusside results in formation of the $[Fe(CN)_5NO]^{3-}$ complex and *S*-nitrosothiol (24).

$$[Fe(CN)_5NO]^{2-} + RSNO^{\bullet-} \rightarrow [Fe(CN)_5NO]^{3-} + RSNO \quad (24)$$

Nitrosothiols are also formed upon reaction of $RSNO^{\bullet-}$ with oxygen or other oxidants, while reaction with $[Fe(CN)_5N(SR)O]^{3-}$ results in the formation of an iron dinitrosyl complex and its dimer ($[Fe(SR)_2(NO)_2]^-$, $[Fe_2(SR)_2(NO)_2]$) [16,55–57]. Finally, the nitrosothiyl radical anion may dissociate yielding thiolate and nitric oxide [16].

$$RSNO^{\bullet-} \rightarrow RS^- + NO^{\bullet} \quad (25)$$

Photolysis of the $[Fe(CN)_5N(SR)O]^{3-}$ complex within 313 and 600 nm in the presence of mercaptosuccinate yields almost equal amounts of the $[Fe(CN)_5SR]^{3-}$ complex and *S*-nitrosomercaptosuccinate as main products with quantum yield ranging from 0.005 to 0.25, depending on irradiation wavelength and the presence of oxygen [55–57]. The addition of nitrite significantly decreases the quantum yield of the Fe^{III} complex but at the same time, the quantum yield of RSNO increases. The $[Fe(CN)_5SR]^{3-}$ complex reacts with nitrite in the presence of excess of the thiolate yielding $[Fe(CN)_5N(SR)O]^{3-}$ with quantitative yield. These observations allow postulating a catalytic cycle for photochemical generation of *S*-nitrosothiols in alkaline solution (Fig. 18).

Although the overall photochemical mode in pentacyanoferrate(II) with NO or N(SR)O has similar character, the presence of the sulfur component significantly shifts the spectroscopic range of photooxidation towards longer wavelengths.

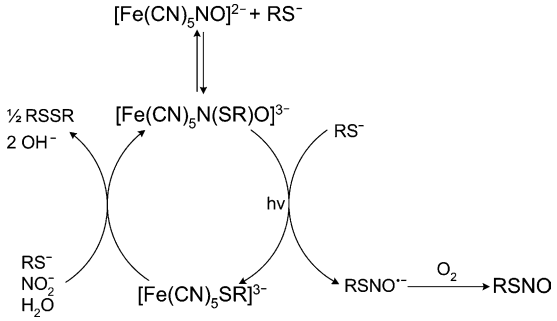

Fig. 18. Catalytic cycle for photochemical nitrosation of mercaptosuccinate. Side reactions were omitted for clarity.

Moreover, the second principal product is now RSNO, instead of NO, as in the case of the Fe–NO system.

7. Ternary systems: Chemistry and photochemistry of compounds with the S–Fe–NO framework

7.1. Biosynthesis of nitric oxide

Nitric oxide can be synthesized on several pathways. Plants use a non-enzymatic strategy in photochemical reaction between NO_2^- and carotenoids or other plant metabolites. The enzymatic pathway involves reduction of nitrite with nitrite reductase and animal-like nitric oxide synthase [256–258]. The most common way of NO synthesis in animal organisms involves a family of enzymes called nitric oxide synthases (NOSs). The biosynthesis of nitric oxide is a good example of mutual interaction of iron centre, thiolate ligand and nitric oxide.

The NOS enzymes are members of the heme-containing super-family of enzymes called monooxygenases [7]. Depending on the structure, expression and activity, the NOS enzymes can be divided into three categories: endothelial NOS (eNOS), neuronal NOS (nNOS) and inducible NOS (iNOS) [1,137,259,260]. The nNOS and eNOS are

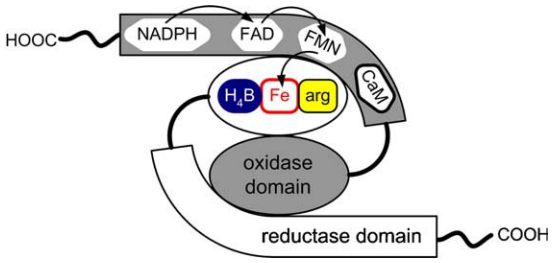

Fig. 19. Schematic structure of nitric oxide synthase dimer. Arrows indicate electron-transfer pathways. Adapted from [264].

involved in maintaining the homeostasis in neural and vascular systems, respectively, while iNOS is expressed in cardiac myocytes, smooth muscle cells and macrophages upon stimulation with cytokines, interferones, endotoxins and inflammatory mediators [7,256,261,262]. The iNOS generates NO in amounts two to three orders of magnitude higher than other NOS isoforms, exerting strong cytotoxic and antimicrobial activity. All these enzymes are composed of two subunits: reductase and oxygenase (Fig. 19). The reductase subunit is very similar to other reductases, e.g. cytochrome *c* reductase. It is located at the C-end of the polypeptide chain and has a modular structure consisting of a series of binding sites for electron donor (NADPH) and flavin molecules (FAD and FMN, Fig. 20), thus creating an electron-transfer chain. The N-end of the protein constitutes the oxygenase unit with binding sites for heme moiety, tetrahydrobiopterin and L-arginine. The structure and properties of oxygenase subunit are closely related to that of cytochrome P450. The iron porphyrin is tethered to the protein backbone via cysteine coordinated to iron as axial ligand. This arrangement is typical for the whole class of cytochrome P450 proteins and is responsible for oxygen activation and stabilization of the oxidized form of the protein. Axial thiolate ligand provides electron density preventing π-back bonding of the oxygen atom [263]. Both domains are connected via Ca^{2+}/calmodulin (CaM)-binding site [264]. The active form of the enzyme is a dimer, in which reductase subunit of one molecule is tightly bound with the oxygenase subunit of the other molecule via a series of hydrogen bonds [259,261,264]. The zinc–cysteine complex, located close to the surface of the protein plays a crucial role in stabilization of the dimeric structure [260]. During NO productions electron transfer occurs from the reductase frag-

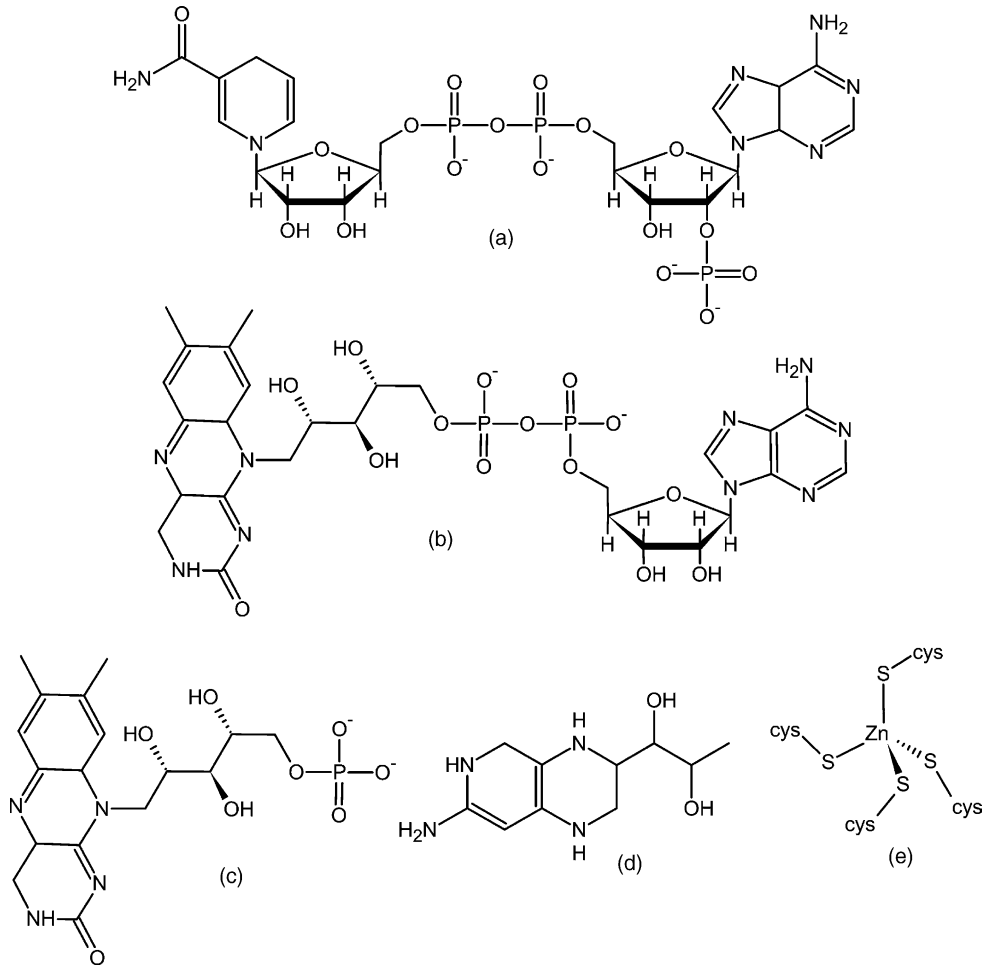

Fig. 20. Nitric oxide synthase cofactors: (a) nicotinamide adenine dinucleotide (NADPH); (b) flavin adenine dinucleotide (FAD); (c) flavin mononucleotide (FMN); (d) tetrahydrobiopterin (H_4B); (e) $[Zn(S\text{-cys})_4]^{2-}$ complex [137].

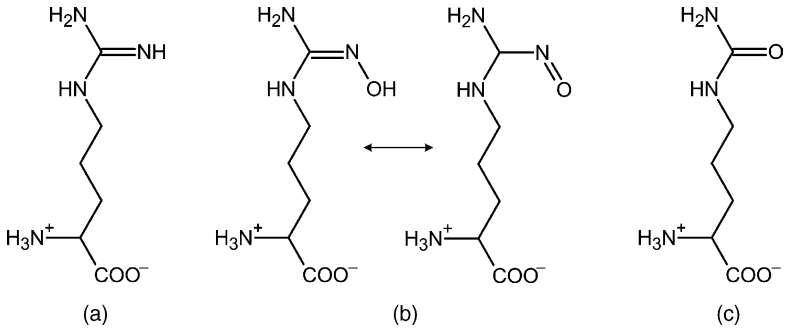

Fig. 21. Molecular structure of arginine (a), *N*-hydroxyarginine (b) and cytruline (c).

ment of one molecule to the oxygenase subunit of the other (Fig. 19) [7,259,261,264–266].

Biosynthesis of nitric oxide requires two catalytic cycles, first oxidizing L-arginine to intermediate *N*-hydroxy-L-arginine and subsequently *N*-hydroxy-L-arginine to cytruline and nitric oxide [7,62,256,259,261,264–267] (Fig. 21). The primary step of NO biosynthesis encompasses reduction of ferric heme, coordination of dioxygen and electron-transfer reactions resulting in overall two-electron reduction of oxygen molecule. Axial thiolate ligand stabilizes highly oxidizing perferryl, $[FeO]^{3+}$, centre (vide infra) [7,263]. The perferryl oxidizes L-arginine via oxygen insertion into the N–H bond within guanidine moiety (Fig. 22) [7,62].

While the mechanism of *N*-hydroxy-L-arginine formation is well-elucidated, much controversy arises around the second oxidation step. The most accepted mechanism assumes two-electron reduction of oxygen with one electron coming from NADPH and the other from *N*-hydroxy-L-arginine. Resulting *N*-hydroxy-L-argininyl cation radical reacts with Fe-coordinated peroxide yielding L-cytruline and nitric oxide [7] (Fig. 22). The exact mechanism of this process is still unclear and is a subject of intense research [7].

Axial coordination of the iron–heme complex in nitric oxide synthase is of crucial importance for proper activity of this enzyme. Numerous oxidoreductases possess iron porphyrin complex containing axially coordinated cysteine or methionine in their active site [7,141,263]. Such structures are found in cytochrome P450-type enzymes [141,217,218,263,268–272] and various siroheme proteins like nitrite reductases and sulfite reductases (cf. Fig. 13h) [159]. These sulfur-containing axial ligands play an important role in stabilizing high-valent iron porphyrin complexes in cytochrome P450-type enzymes. Electron-rich sulfur centre together with porphyrin ligand stabilizes ferryl (FeO^{2+}) moiety due to resonance (Fig. 23) [141,263] and thus enhances its electrophilicity, which is crucial for enzymatic activity of these species [270]. DFT calculations indicate that the sulfur ligand possesses partial radical character [268,271,272], which supports the resonance model. This illustrates the astonishing but general tendency of sulfur-

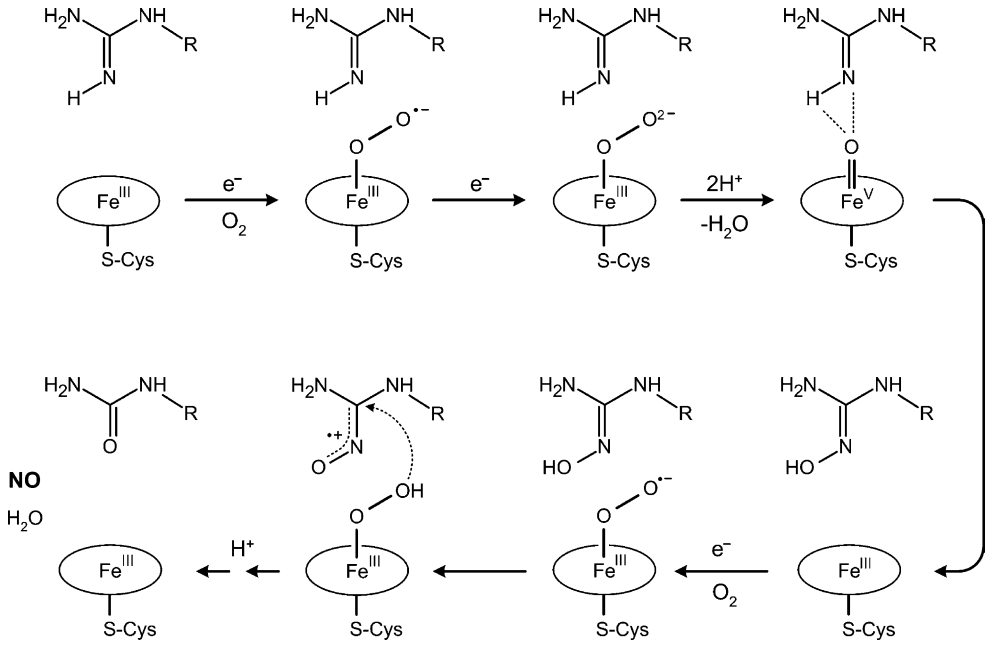

Fig. 22. General mechanism of NO biosynthesis catalyzed by nitric oxide synthase. Based on Refs. [7,62,264,266].

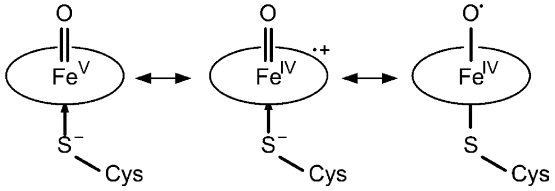

Fig. 23. Resonance stabilization of the ferryl ion with contribution of porphyrin and thiolate axial ligand [263].

containing ligands to stabilize high oxidation states of transition metals [216,273].

7.2. Other biochemical systems utilizing the S–Fe–NO framework

One of the most important physiological processes is oxygen delivery to cells and tissues. One theory assumes an important role of nitrosyl transfer between heme iron and β93 cysteine of hemoglobin. It was assumed that allosteric changes of the protein may induce NO release from nitrosothiol moiety thus increasing blood flow in hypoxic tissues [238,274]. Some recent work, however, does not support this hypothesis [275–279]. The process is undoubtedly very important but its understanding requires further research.

Reduction of nitric oxide can be catalyzed by nitric oxide reductase ($P450_{nor}$), an enzyme closely related to nitric oxide synthase [97,280,281]. This unusual enzyme, despite structural analogy to cytochrome P450, cannot activate molecular oxygen. Instead it binds nitric oxide and reduces it to N_2O. The proposed mechanism includes several steps and intermediates, which are stabilized via resonance. In the first step nitric oxide is bound to the Fe^{III} heme centre. The complex is stabilized by two resonance forms Fe^{II}–NO^+ and Fe^{IV}–NO^-. Two-electron reduction by NADH and addition of two protons yield Fe^{III} centre with coordinated hydroxylamine radical. Addition of nitric oxide yields an intermediate, which produces N_2O and water (Fig. 24) [97,280,281]. As in the case of nitric oxide synthase, the high-valent iron centres are stabilized by interaction with axial cysteine.

Nitrite reductase is another example of a complex enzymatic system involving mutual interactions in iron–nitrosyl–sulfur system. The active site of the enzyme contains iron ion coordinated inside a siroheme macrocycle coupled with Fe_4S_4 core via cysteine bridge [97,282]. Substrate (NO_2^-) binds to the porphyrin iron and the iron–sulfur cluster served as an electron reservoir. The detailed mechanism of the process remains unclear, but nitrosyl, nitroxyl and hydroxylamine complexes were identified as intermediates [282].

Nitrophorins are a group of proteins found in the saliva of two species of blood-sucking insects, kissing bug (*Rhodnius prolixus*) [239–243] and a bedbug (*Cimex lectularius*) [283–285]. The latter one is especially interesting, as it involves both heme iron and a proximal cysteine for nitric oxide storage and can store (and transfer) two NO molecules within one protein molecule. NO-binding involves two steps. First NO is bound to Fe^{III} heme yielding an unstable intermediate complex. Reaction with a second NO molecule accompanied with electron transfer yields the stable Fe^{II} nitrosyl complex and *S*-nitrosothiol moiety (Fig. 25) [284,285].

An unique iron–sulfur–nitrosyl complex was found in the active site of nitrile hydratase [286]. Nitrile hydratases are hydrolytic enzymes responsible for the sequential metabolism of nitrile compounds in some bacteria and fungi, which are capable of utilizing aliphatic nitriles as the sole source of nitrogen and carbon. Nitrile hydratases are mononuclear iron or (non-corrinoid) cobalt enzymes that catalyze hydration of a large number of diverse nitriles to their corresponding amides. These enzymes have been efficiently used for the industrial production of acrylamide from acrylonitrile and for removal of nitriles from wastewater [287,288].

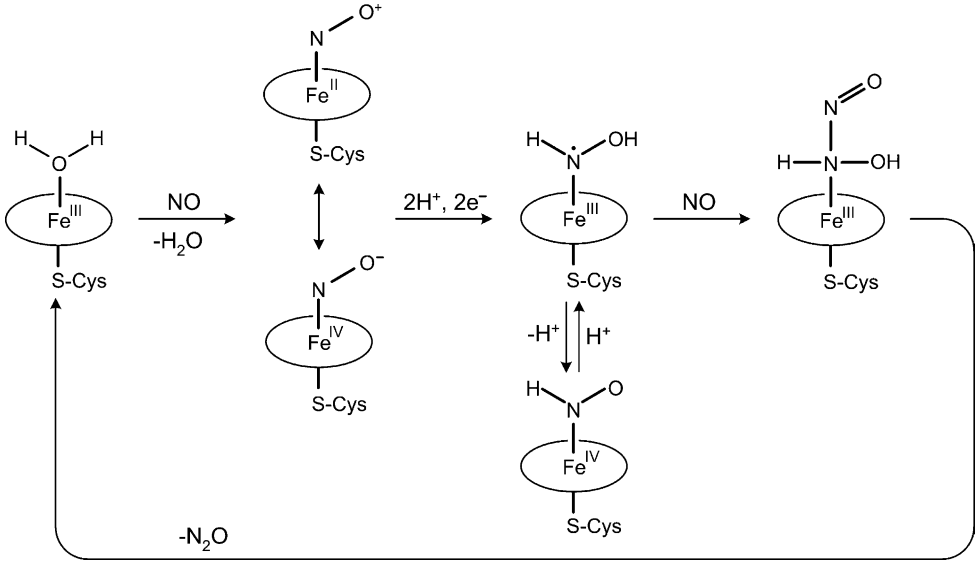

Fig. 24. Proposed mechanism for nitric oxide reduction with $P450_{NOR}$. Adapted from [97,280,281].

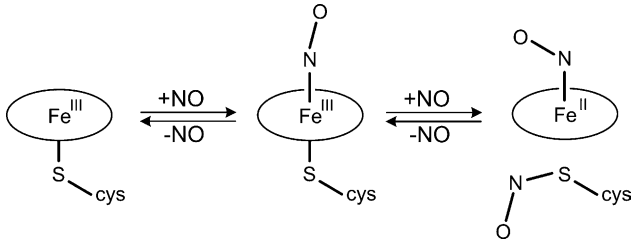

Fig. 25. Proposed mechanism for reversible NO-binding by *Cimex lectularius* nitrophorin. Adapted from [284,285].

The active site of these enzymes contains a low spin Fe^{III} centre. The first coordination sphere consists of two amide nitrogen atoms from protein skeleton and three sulfur atoms from cysteine. Two of the three-cysteinate ligands are modified; the active form of the enzyme contains one sulfenic (cys-SOH) and one sulfinic (cys-SO_2H) form of cysteine (cf. Fig. 5). The sixth coordination site is occupied by a water molecule or hydroxide anion (in the active form of the enzyme) or nitric oxide (in the inactive form) [289,290]. Light is an essential factor regulating activity of nitrile hydratase. In the dark, active enzyme is deactivated by nitric oxide, while irradiation of the inactive form results in photosubstitution, which restores the enzyme's activity [291].

Due to their industrial importance, the systems mimicking nitrile hydratase have been extensively studied [231,292–297]. These model compounds can reproduce spectroscopic properties of the enzyme [231,293], some of them are able to reversibly bind nitric oxide (to iron ion) [295,296] or oxygen (to sulfur atoms) [295]. Recently, a model compound-binding reversible nitriles has been found [294]. Some of these compounds are closely related to Roussin's red esters (vide infra) [296].

7.3. Chemistry and photochemistry of iron–sulfur–nitrosyl clusters

The first iron–sulfur–nitrosyl clusters ever synthesized were nitrosylthiolatoferrates [298–300]. In contrast to clusters containing solely terminal thiolate ligands, these nitrosyl complexes are usually air and moisture stable compounds [213]. They are known to form both mononuclear complexes and clusters containing two-, three-, four- and six-iron centres, which are recognized or considered, to play a role of NO-donor in biomedical systems [90,213,301–304]. The complexes are reported to act as NO-donor drugs and they are also generated under (patho)physiological conditions (e.g. during nitrosative stress or when relatively high doses of iron and nitrite are supplied with food); some of them, e.g. $[Fe_2(\mu_2\text{–}SCH_3)_2(NO)_4]$, can be found in natural sources [9,301,305]. The food-preserving properties of nitrate and nitrite are also associated with formation of iron–sulfur–nitrosyl species showing extreme toxicity towards anaerobic food spoilage bacteria (e.g. *Clostridium botulinum*) [306,307].

The interaction of NO with the natural [Fe–S] clusters gives rise to the iron–sulfur cluster nitrosyl complexes [71]. These include: $[Fe_2(\mu_2\text{–}S)_2(NO)_4]^{2-}$ (dianion of 'Roussin's red salt', RRS), $[Fe_2(\mu_2\text{–}SR)_2(NO)_4]$ (Roussin's red esters, RRE, R = alkyl or aryl), $[Fe_4(\mu_3\text{–}S)_3(NO)_7]^-$ (heptanitrosyltri-μ_3–sulfido-tetraferrate, 'Roussin's black salt' anion, RBS), $[Fe_4(\mu_3\text{–}S)_4(NO)_4]$ (tetranitrosyl-tetra-μ_3-sulfidotetrahedro-tetrairon, 'cubane') and other cubane-like clusters like $[Fe_4(\mu_3\text{–}S)_2(\mu_3\text{–}NCMe_3)_2(NO)_4]$ and $[Fe_4(\mu_3\text{–}S)_3(NO)_4(PR_3)_3]$. Clusters of higher nuclearity, e.g. $[Fe_6(\mu_3\text{–}S)_6(NO)_6]^{2+}$ were also reported [210,308] (Fig. 14). The compounds occur in a variety of geometrical forms, containing different numbers of metal centres, varied Fe:NO:S ratios and various co-ligands, a number of factors can influence their proneness to behave as the NO-carriers. Interactions with solvents and external ligands easily leads to the interconversion of clusters (Fig. 26). The bond lengths and angles are quite similar in all the clusters within this family (Table 4).

7.3.1. Mononuclear nitrosylthiolatoferrates

The family consists of the tetrahedral $[Fe(SR)_x(NO)_{4-x}]^-$ complexes, where $x = 2$ or 3. Those with $x = 2$ are known as responsible for storage and transport of NO in biological tissues and their trivial name is dinitrosyl iron complexes (DNICs) [301]. Their chemical reactivity and spectroscopic characteristics have been studied in some detail [55,56,301,311,312,317–319].

All $[Fe(SR)_2(NO)_2]^-$ and other $[FeL_2(NO)_2]^-$ complexes are paramagnetic, their EPR spectra depend only slightly on the ligand structure and can be regarded as a fingerprint for this class of compounds (Table 5). The $g_{||} < g_\perp$ indicates that the ground state is largely confined to d_{z^2} orbital [56].

Recently, these properties were interpreted using density functional calculations [66]. The DFT calculations confirmed the experimentally measured integral spin value of $S = 1/2$ [55,56,301,311,312,317–319]. Moreover, the low spin configuration, not typical for the tetrahedral or pseudotetrahedral complexes, finds its interpretation in the antiferromagnetic coupling between the Fe^{III} centre and the NO^- ligands. The description of the iron centre as Fe^{III} or Fe^{-I} is, however, simplistic, as the calculated spin densities point at the former, whereas the net chemical behaviour is consistent with the latter approximation.

The $[Fe(SR)_2(NO)_2]^-$ complexes are reactive species, whose stability in solution is maintained only in the presence of a large excess of RS^- [56,301,311,312,317–319]. Otherwise, the ions readily undergo condensation to a dinuclear structure via formation of two RS-bridges and release other two RS^- ligands in the reversible reaction:

$$2[Fe(SR)_2(NO)_2]^- \rightleftarrows [Fe_2(\mu_2\text{–}SR)_2(NO)_4] + 2RS^- \quad (26)$$

The DFT calculations [66] allowed one to understand the tendency to form the double-bridged species (Eq. (26)). The HOMO orbitals of $[Fe(SR)_2(NO)_2]^-$ are mostly localized at

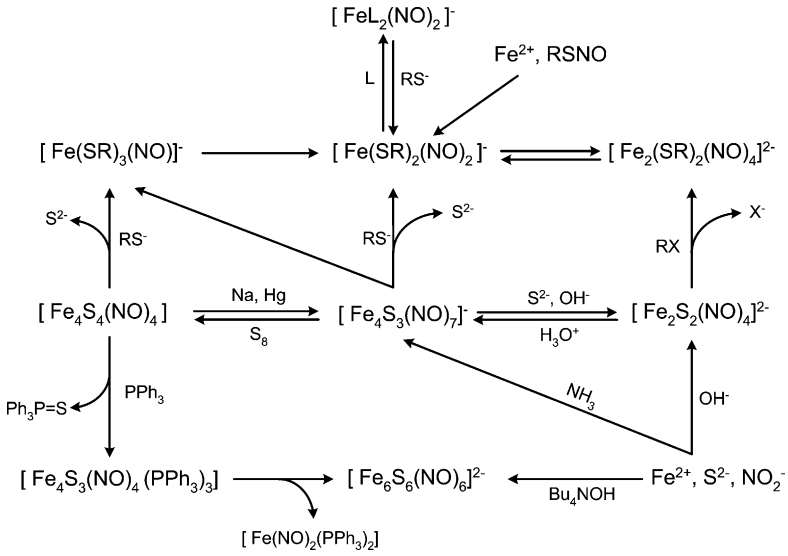

Fig. 26. Thermal transformations of iron–sulfur nitrosyl complexes and clusters [213,309–312].

the sulfur atoms with a large space extent, whereas LUMO's are mainly of the d character; thus, the effective overlap of the orbitals of two entities can result in formation of the first RS-bridge. The distorted tetrahedral geometry of the complex [317] as well as polarization of the S–C bond enhanced in the polar solvent can favour the step. The next reaction step, i.e. formation of the second RS-bridge and release two RS^- ligands may be realized in a concerted process.

The $[Fe(SR)_2(NO)_2]^-$ complexes are able, as well, to transfer its NO-ligands to other molecules, e.g. to thiol distinct from that coordinated to the iron centre. In such a case the thiol *S*-nitrosation could be observed.

$$[Fe(SR)_2(NO)_2]^- + R'SH \rightarrow R'S{-}NO + \text{decomposition products} \quad (27)$$

The reaction (27) was documented for the systems, where RS = L-cysteine or GSH and R′S = albumin) [301,318]. This behaviour is responsible for the role of the $[Fe(SR)_2(NO)_2]^-$ complexes in NO-storage and NO-transport occurring in vivo [301]. The DFT calculations [66] have shown that in the polar solvent the charge separation within the NO-ligands is significant. In consequence, the charge localized on the N-atom becomes more positive enabling a nucleophilic attack, which is known to initiate nitrosation in the case of numerous nitrosyl complexes [55,56,213,312]. A considerable contribution of the π^*_{NO} to the LUMO orbitals assists the attack and enables the consecutive Fe–NO bond cleavage.

Although experimental data for the $[Fe(SR)_3(NO)]^-$ complexes are scarce, behaviour similar to that of $[Fe(SR)_2(NO)_2]^-$ can be expected, based on the DFT cal-

Table 4
Structural parameters for various Fe—S—NO clusters

Compound	Crystallographic parameters						References
	Bond lengths (Å)			Bond angle (°)			
	Fe–N	Fe–S	N—O	Fe—N—O	Fe—S—Fe	S—Fe—S	
$[Fe(SR)_3NO]^-$ [a]	1.684	2.319	1.188	157.4	–	109.7	[66]
$[Fe(SR)_2(NO)_2]^-$ [a]	1.655	2.273	1.165	169.8	–	109.2	[66]
$[S_5Fe(NO)_2]^-$	1.678	2.287	1.177	165.9	–	107.7	[214]
$[Fe_2(\mu_2{-}S)_2(NO)_4]^-$ [a]	1.618	2.266	1.208	163.2	73.7	106.3	[330]
$(Me_4N)_2[Fe_2(\mu_2{-}S_2O_3)_2(NO)_4]$	1.669	2.258	1.16	169.6	73.59	106.4	[313]
$[Fe_2(\mu_2{-}SR)_2(NO)_4]$	1.67	2.27	1.17	167.8	74	106	[314]
$[Fe_4(\mu_3{-}S)_4(NO)_4]$	1.663	2.217	1.155	177.6	73.43	109.37	[212]
$[Fe_4(\mu_3{-}S)_4(NO)_4]^-$	1.659	2.231	1.168	177.5	74.33	103.62	[212]
$[Fe_4(\mu_3{-}S)_3(NO)_7]^-$	1.667	2.241	1.161	178.3[b] 166.4[c]	74.34	105.62	[315]
$[Fe_4(\mu_3{-}S)_3(NO)_7]^{2-}$	1.646	2.249	1.176	177.6[b] 167.9[c]	75.79	104.18	[315]
$[Fe_6(\mu_3{-}S)_6(NO)_6]^{2-}$	1.665	2.219	1.184	174.1	73.12	108.88	[210]
$[Fe_4(\mu_3{-}S)_2(\mu_3{-}NCMe_3)_2(NO)_4]$	1.661	2.223	1.165	178.4	71.63	104.05	[316]
$[Fe_4(\mu_3{-}S)_2(\mu_3{-}NCMe_3)_2(NO)_4]^-$	1.608	2.254	1.208	176.5	71.85	101.9	[316]

[a] From DFT calculations.
[b] In axial position.
[c] In equatorial or basal position.

Table 5
Experimental EPR parameters of various $[FeL_2(NO)_2]^{n-}$ complexes [56]

Ligands	77 K		Room temperature			References
	$g_\perp$	$g_{\|\|}$	g_{iso}	A_{iso} (^{14}N)	A_{iso} (^{1}H)	
Mercaptosuccinate	2.0406	2.0120	2.0295	2.42	0.97	[56]
Glutathione	2.04	2.01	–	–	–	[320]
Cysteine	2.04	2.01	–	–	–	[321]
Cysteine	2.039	2.013	2.028	1.2	1.2	[322]
$(CH_3)_2CHS^-$	–	–	2.028	2.5	0.5	[322]
$(CH_3)_2CHS^-$	–	–	2.027	2.5	1.3	[213]
$CH_3CH_2CH(CH_3)S^-$	–	–	2.028	2.5	0.5	[322]
HS^-	–	–	2.028	2.7	0.5	[213]
CH_3S^-	–	–	2.028	2.1	2.1	[213]
$(CH_3)_3CS^-$	–	–	2.027	2.7	–	[213]
$C_6H_5CH_2S^-$	–	–	2.027	2.4	1.4	[213]
$CH_3CH_2CH_2S^-$	–	–	2.028	1.2	1.2	[322]
$CH_3CH_2CH_2CH_2S^-$	–	–	2.028	1.2	1.2	[322]
$CH_3(CH_2)_{10}CH_2S^-$		–	2.028	1.2	1.2	[322]
$HOCH_2CH_2S^-$	–	–	2.028	1.2.	1.2	[322]
Homocysteine	–	–	2.028	1.2	1.2	[322]
2-Mercaptobenzimidazole-*S*	2.039	2.013	2.028	2.5	–	[322]
2-Mercaptobenzimidazole-*N*	2.040	2.012	2.029	2.5	–	[322]
2-Mercaptobenzoxazole-*S*	2.040	2.013	2.029	∼2	–	[322]
1,2,3-Benzotriazole	–	–	2.027	2.5	–	[322]
DMF	–	–	2.033	2.4	4.0	[213]
DMF, $(CH_3)_2CHS^-$	–	–	2.027	2.6	1.3, 4.6	[213]
DMA	–	–	2.033	2.5	–	[213]
DMA, $(CH_3)_2CHS^-$	–	–	2.027	2.5	1.3	[213]
Pyridine	–	–	2.031	2.2, 4.5	–	[213]
DMSO, CH_3S^-	–	–	2.032	6.0	3.2	[213]
2,6-Dimethylpyridine	–	–	2.031	2.3, 4.6	–	[213]
Quinoline	–	–	2.032	2.2, 4.4	–	[213]
$(CH_3CH_2)_2NH$, CH_3S^-	–	–	2.030	4.0	2.0	[213]
Pyrrolidine, CH_3S^-	–	–	2.029	4.2	2.0	[213]
Piperidine, CH_3S^-	–	–	2.029	4.2	2.1	[213]
Pyrrolidine, $C_6H_5CH_2S^-$	–	–	2.029	4.2	2.0	[213]

Abbreviations: DMF, dimethylformamide; DMA, dimethylacetamide; DMSO, dimethylsulfoxide.

culations [66]. In this complex, similarly, as in DNICs, the integral spin is reduced due to antiferromagnetic coupling between the iron centre and the NO-ligand, the tetrahedral geometry is strongly distorted and polar solvent exerts a significant impact on ligand polarities. Thus, the negative charge is mostly localized on the oxygen atom of the NO-ligand and DFT calculation showed a moderate positive charge on the nitrogen atom. A slightly longer Fe–N distance and smaller Fe–N–O angle, than in the DNICs, may point at some stronger contribution of the Fe^{III}–NO^- structure, and in consequence, a slightly weaker nitrosation capacity the $[Fe(SR)_3(NO)]^-$ complexes, although it should not entail a meaningful difference in the chemical reactivity.

Calculations of electronic spectra [66] revealed that all bands of the $[Fe(SR)_x(NO)_{4-x}]^-$ complexes are of the CT-type, whose character changes with the increase in the transition energy from LLCT ($S_\pi \rightarrow \pi^*_{NO}$) + LMCT ($S_\pi \rightarrow d$) to LMCT ($\pi^*_{NO} \rightarrow d + S_\pi \rightarrow d$) and at last to MLCT ($d \rightarrow \pi^*_{NO}$). It may then be presumed that the effectiveness of nitrosation should be enhanced upon irradiation. This hypothesis needs, however, requires experimental verification.

7.3.2. Dinuclear complexes

The family of dinuclear iron–sulfur–nitrosyl complexes includes: $[Fe_2(\mu_2\text{–}S)_2(NO)_4]^{2-}$ (dianion of 'Roussin's red salt', RRS) (Fig. 14a), $[Fe_2(\mu_2\text{–}SR)_2(NO)_4]$ (Roussin's red esters, RRE, R = alkyl or aryl) and complexes, where bridging sulfide serves as a ligand to other transition metal ions, like Ni^{2+}, Pt^{2+} or Hg^{2+} [324,325]. Some dimeric iron nitrosyls with extended bridging ligand based on the N–C–S framework were also reported [326].

The $[Fe_2(\mu_2\text{–}S)_2(NO)_4]^{2-}$ anion (RRS) is stable in alkaline medium, whereas in acidic medium, it undergoes an electrophilic attack generating protonated intermediates $[Fe_2(\mu_2\text{–}S)(\mu_2\text{–}SH)(NO)_4]^-$ and $[Fe_2(\mu_2\text{–}SH)_2(NO)_4]$ [245,327], which aggregate readily yielding the poly-nuclear cluster structures: $[Fe_4(\mu_3\text{–}S)_3(NO)_7]^-$, $[Fe_5(\mu_3\text{–}S)_4(NO)_8]^-$ or $[Fe_7(\mu_3\text{–}S)_6(NO)_{10}]^-$ [245,301,305]. The aggregation reactions are accompanied by the formal release from the initial RRS of one S^{2-} and 1, 2 or 4 NO^- ligands for tetra-, penta-, and hepta-nuclear species, respectively. RRS is also well known to react readily with halogenoalkanes, and this reaction has been extensively exploited for the synthesis of

the RRE [328,329]. It reacts also with nickel, platinum and mercury complexes yielding multinuclear heterometallic compounds [324,325].

A theoretical analysis [330] gives a good account of this behaviour. The electrophilic attack, which initiates the RRS reactivity, takes place on the bridge sulfur atoms. This assumption is consistent with the character of the HOMO orbitals, which are mostly localized on the S-atoms. Association of the electrophile is facilitated by the negative charges of both sulfur atoms in RRS.

Photochemical reactivity of $[Fe_2(\mu_2\text{–}S)_2(NO)_4]^{2-}$, upon 355-nm excitation, leads in the presence of O_2 to generation of $[Fe_4(\mu_3\text{–}S)_3(NO)_7]^-$. Although the photoproduct is the same as product of the thermal reaction, mechanism of the photoreaction suggested from the flash experiments is quite different [88,331]. The photochemical aggregation is initiated by dissociation of one of the NO groups and formation of the $[Fe_2(\mu_2\text{–}S)_2(NO)_3]^{2-}$ intermediate. The DFT calculations show that the transitions ascribed to the band at 374 nm in the experimental spectrum are mostly of the $\pi^*_{NO} \rightarrow$ d LMCT character with admixture of the minor d $\rightarrow \pi^*_{NO}$ transitions. Thus, the reactive decay of the states should lead readily to the Fe–NO bond cleavage.

Opposite to RRS, the $[Fe_2(\mu_2\text{–}SR)_2(NO)_4]$ esters are known to undergo a nucleophilic attack on the bridge S atoms, which leads to ring-opening and formation of mononuclear paramagnetic complexes. In the presence of the thiolate anions, this reaction results in formation of the monomeric $[Fe(\mu_2\text{–}SR)_2(NO)_2]^-$ complexes (28).

$$[Fe_2(\mu_2\text{–}SR)_2(NO)_4] + 2RS^- \rightleftarrows 2[Fe(SR)_2(NO)_2]^- \quad (28)$$

Alternatively, the ring-opening can be followed by a rapid substitution of both RS^- ligands by other nucleophilic anions or solvent molecules, generating the sporadically detectable mono-substituted $[Fe(\mu_2\text{–}SR)X(NO)_2]^-$ intermediates, which are transformed into the stable di-substituted $[FeX_2(NO)_2]^-$ complexes (where X = Br^-, I^-, SCN^-, N_3^-, NCO^-, NO_2^-, DMF, DMSO) [301,311] (cf. Table 4).

$$[Fe(\mu_2 - SR)X(NO)_2]^- \xrightarrow[-RS^-]{X} [Fe(\mu_2 - SR)X(NO)_2]^- \xrightarrow[-RS^-]{X} [FeX_2(NO)_2]^- \quad (29)$$

The nucleophilic attack engages the LUMO orbital, which is mostly localized on the Fe and S atoms [330]. Association of a nucleophile is facilitated by the positive charges of both the S atoms in RRE. Splitting of the S-bridges, which follows the nucleophilic attack and leads to formation of the monomeric $[FeX_2(NO)_2]^-$ complexes (Eq. (29)), is substantiated by the antibonding Fe–S character of the LUMO orbital, as well as by the relatively long Fe–S bond in RRE (227 pm).

In thermal reactions, the Fe–NO bond in $[Fe_2(\mu_2\text{–}SR)_2(NO)_4]$ is inactive, and thus, its role in promoting the carcinogenic properties of other substances [305] can be substantiated only by its initial transformation into the $[Fe(SR)_2(NO)_2]^-$ monomers in reaction with the thiolates present in the human body (Eq. (28)), followed by nitrosothiols production (Eq. (27)).

The quite different reactivity of the Fe–NO bond is demonstrated, when RRE solutions are excited by 355 nm radiation [323]. Then RRE undergoes photodissociation of the NO group, followed (in aerated medium) by a complete decomposition. Such behaviour is substantiated by the DFT method [330]: excitation by radiation within the 370-nm band, assigned to the d $\rightarrow \pi^*_{NO}$, $\pi^*_{NO} \rightarrow \pi^*_{NO}$ and $\pi^*_{NO} \rightarrow$ d transitions, should result in a weakening, and in consequence cleavage, of the Fe–NO bond.

The contrasting chemical behaviour of RRS and RRE, which are structurally similar species, finds its explanation in charge distributions and character of their frontier orbitals. The most outstanding difference in charge distribution concerns the sulfur atoms, which are negative in RRS, and positive in RRE. This distinction is reflected in their opposite susceptibility to undergo an electrophilic/nucleophilic attack. In accordance with this, the character of the frontier orbitals favours the electrophilic attack in the case of RRS, whereas the nucleophilic attack in the other case. Contrary to the mononuclear $[Fe(SR)_x(NO)_{4-x}]^{n-}$ complexes ($x = 2$ or 3), the dinuclear clusters do not reveal a tendency for the homolytic cleavage of the Fe–NO bond in thermal reactions. The behaviour is substantiated by a higher charge on the N-atoms in the former case, enabling the cleavage via a nucleophilic attack [332]. They can, however, behave as indirect NO-donors due to reactivity of the products of their thermal reactions, which split easily the Fe–NO bonds: i.e. RBS in the case of RRS and the $[Fe(SR)_2(NO)_2]^-$ monomer for RRE.

Both dinuclear complexes demonstrate, however, similar photochemical reactivity consisting in photodissociation of the NO group, because in both cases, the transition responsible for the photochemical reactivity is of the $\pi_{NO} \rightarrow$ d LMCT character. Similar behaviour was recently observed for the supramolecular system containing the dimeric $[Fe(\mu_2\text{–}SR)_2(NO)_2]$ moiety linked with protoporphyrin IX chromophore. Near infrared irradiation of this compound within the absorption of the porphyrin chromophore results in nitric oxide liberation in two-photon process [333,334].

The different reactivity of the RRS and RRE dinuclear species has its origin in the differences in charges localized on the bridging S atoms. This illustrates well the versatility of the (S–Fe–NO) moiety, in which charge shift between the S atom and NO group through the Fe-centre can happen readily, changing the nucleophilic or electrophilic character of these ligands.

7.3.3. Tetranuclear clusters

Among the iron–sulfur–nitrosyl complexes, there are also tetranuclear clusters $[Fe_4(\mu_3\text{–}S)_3(NO)_7]^-$ ('Roussin's black salt' anion, RBS, Fig. 14b), $[Fe_4(\mu_3\text{–}S)_4(NO)_4]$

(tetranitrosyl-tetra-μ_3-sufidotetrahedro-tetrairon, 'cubane', Fig. 14c), $[Fe_4(\mu_3–S)_2(\mu_3\text{-}NCMe_3)_2(NO)_4]$ and $[Fe_4(\mu_2–S)_3(NO)_4(PR_3)_3]$. The most important and the best recognized is RBS, whose structural, photochemical and reactivity properties have been widely investigated [245,315,335–337].

The geometry of RBS (Fig. 14b) shows that four Fe-atoms are bound by three μ_3-sulfur bridges and coordinated terminal NO-ligands. The cluster consists of three $[Fe(\mu_3–S)_2(NO)_2]$ constitutional units (basal Fe atoms), whereas one of the Fe-atoms (apical Fe1 atom) is distinguished by its direct coordination sphere, which is $[Fe(\mu_3–S)_3NO]$. The structural difference is reflected in the Fe–N–O angles, which for the apical Fe1 atom are more close to 180°, than in the other cases [315,337], suggesting the highest contribution of the NO^+ form in the NO bonded to Fe1 (Table 4).

RBS may be viewed as composed of $\{Fe(NO)\}^7$ unit with $S = 3/2$ antiferromagnetically coupled to three $\{Fe(NO)_2\}^9$ units with $S = 1/2$ giving a total spin of the molecule $S = 0$. In the $\{Fe(NO)\}^7$ unit, the Fe^{3+} ($S = 5/2$) ion is antiferromagnetically coupled to one NO^- ion ($S = 1$), which leads to $S = 3/2$ of the fragment, in $\{Fe(NO)_2\}^9$ high spin ferric ion is antiferromagnetically coupled to two NO^- ($S = 1$) ions, which leads to spin $S = 1/2$ [338].

In the dark, the $[Fe_4(\mu_3–S)_3(NO)_7]^-$ solutions are stable, provided that the pH is not very high. Otherwise, the RBS decomposition to dinuclear RRS is observed [213].

$$[Fe_4(\mu_3 - S)_3(NO)_7]^- \xrightarrow{OH^-} [Fe_2(\mu_2 - S)_2(NO)_4]^{2-} \quad (30)$$

This behaviour can be interpreted in terms of a nucleophilic attack of the OH^- ion on the NO-ligand coordinated to Fe1, which seems to have a major contribution of the NO^+ form, not only due to the Fe–N–O angle close to 180° but also because its N-atom charge, which is somewhat less negative, than in the remaining NO-ligands [338]. On the other hand, the LUMO orbitals are spread over all the Fe atoms and on the basal, not apical, NO-ligands, what could rationalize the nucleophilic attack on any of the NO-ligands [338]. The nucleophilic attack should be followed by cleavage of some of the Fe1–μ_3–S bonds and formation of the second μ_3–S bridge between two other Fe atoms.

The $[Fe_4(\mu_3–S)_3(NO)_7]^-$ cluster is susceptible as well towards nucleophilic attack on Fe–S bonds. As a result, the monomeric complexes of the structure $[Fe(SR)_3NO]^-$ and $[Fe(SR)_2(NO)_2]^-$ are formed according to Eq. (31) [312]. Sulfide ligands are replaced with thiolates, while nitrosyl ligands remain unchanged (Fig. 26).

$$[Fe_4(\mu_3–S)_3(NO)_7]^- + 9RS^- \rightarrow 3[Fe(SR)_2(NO)_2]^- + [Fe(SR)_3NO]^- + 3S^{2-} \quad (31)$$

The $[Fe(SR)_2(NO)_2]^-$ complex originates from basal iron atoms, while the $[Fe(SR)_3NO]^-$ is formed form the apical one. A similar type of reactivity was observed for the $[Fe_4(\mu_3–S)_4(NO)_4]$ complex (32).

$$[Fe_4(\mu_3–S)_4(NO)_4] + 12RS^- \rightarrow 4[Fe(SR)_3NO]^- + 4S^{2-} \quad (32)$$

As the behaviour resembles that observed for the RRE, its interpretation could be analogous.

The $[Fe_4(\mu_3–S)_3(NO)_7]^-$ complex undergoes two consecutive, reversible one-electron reductions, yielding relatively unstable $[Fe_4(\mu_3–S)_3(NO)_7]^{2-}$ and $[Fe_4(\mu_3–S)_3(NO)_7]^{3-}$ complexes [315]. Reduction populates an antibonding orbital of the cluster, which results in elongation of the Fe–S bonds and distortion of the core resulting in symmetry change from C_{3v} to C_s. The $[Fe_4(\mu_3–S)_4(NO)_4]$ complex also undergoes two reversible one-electron reductions yielding corresponding mono- and di-anions: $[Fe_4(\mu_3–S)_4(NO)_4]^-$ and $[Fe_4(\mu_3–S)_4(NO)_4]^{2-}$ [212]. Reduction of the cubane cluster induces analogous bond length and symmetry changes as that observed in the case of RBS: while the $[Fe_4(\mu_3–S)_4(NO)_4]$ cluster has perfect tetrahedral T_d symmetry, anionic form is significantly distorted to D_{2d} [212]. The Fe–S distances are somewhat longer, as the antibonding orbital localized at the Fe_4 core is partially occupied (Table 4).

Oxidation of the $[Fe_4(\mu_3–S)_3(NO)_7]^-$ anion results in complete destruction of the cluster core, the only exception is observed in the case of oxidation with elemental sulfur, when the reaction in toluene yields the $[Fe_4(\mu_3–S)_4(NO)_4]$ cubane complex [310].

The synthesis of novel mixed-ligand clusters involves reactions of the cubane $[Fe_4(\mu_3–S)_4(NO)_4]$ cluster with triphenylphosphine [309]. Reductive desulfurization of the Fe_4S_4 core yields the incomplete cubane core Fe_4S_3 coordinated with phosphine and nitrosyl ligands. The structure of these compounds resembles that of RBS-containing phosphine ligands in place of equatorial nitrosyls. The $[Fe_4(\mu_3–S)_3(NO)_4(PR_3)_3]$ complex undergoes thermal decomposition yielding stable prismane cluster complex $[Fe_6(\mu_3–S)_6(NO)_6]^{2-}$ [308] (cf. Fig. 26).

The photochemistry of $[Fe_4(\mu_3–S)_3(NO)_7]^-$ was studied repeatedly and complete photodegradation of the cluster to its components was observed during continuous irradiation of aerated aqueous solution [88,335]:

$$[Fe_4(\mu_3 - S)_3(NO)_7]^- \xrightarrow{h\nu} 3.9Fe^{2+} + 5.9NO + 3S^{3-} + ? \quad (33)$$

The flash photolysis study with time-resolved optical and infrared spectroscopic techniques revealed two separate intermediates, which both react with nitric oxide. The products were interpreted in terms of photodissociation either the apical or one of the basal nitrosyls from the excited $[Fe_4(\mu_3–S)_3(NO)_7]^-$ entity [335].

Results of recent DFT calculations [338] have shown that excitation within 350–370 nm should lead mostly to charge

transfer from the RBS moiety to the apical NO, whereas excitation within 290–320 nm results in charge transfer directed towards basal and axial NO-ligands. These charge transfers could be responsible for weakening the relevant bonds and dissociation of apical and basal (or equatorial) NO-ligands, respectively.

Attempts to calculate the structures of the oxidized forms of the photoproducts were unsuccessful, showing their high instability [338]. This is consistent with the conception of their formation and prompt decomposition in the presence of molecular oxygen, which would be responsible for the RBS photodecomposition under these conditions [335]. Similar instability found for RBS upon its one electron oxidation suggests, however, that other photochemical pathways cannot be excluded [65].

8. Concluding remarks

This review shows that the very rich chemistry of iron–sulfur–nitrosyl systems has its source in the unique properties of sulfur and nitric oxide ligands as well as in the high affinity of these ligands to coordinate to the iron centre. Co-operative interactions in binary (iron–sulfur, iron–nitrosyl and sulfur–nitrosyl) and especially, in ternary systems are the basis for numerous biochemical processes.

The ternary systems built from both RS–Fe–NO and the FeN(SR)O moieties are unusually flexible due to considerable delocalization of their bonds. This feature results in the unique versatility of the RS–Fe–NO and the FeN(SR)O systems, which can be readily adapted to any chosen function. Even starting from one type of their structure one can “fine tune” using selected organic components since both species are sensitive to the nature of the organic group R. In fact, the influence is not equal, being relatively weak in the RS–Fe–NO systems, and much more pronounced for the FeN(SR)O species. In the latter case, the nature of R appears to be of crucial relevance to the stability of the compound. As a consequence, small structural changes in the R group provide substantial changes in the FeN(SR)O lifetime.

The reactivity of both ternary systems can be also modified by relatively low energy radiation. This is a consequence of the relatively low energies of the charge transfer transitions in these complexes (MLCT, LMCT and/or LLCT) following from considerable delocalization of their molecular orbitals. This feature creates an additional possibility for easy control of the reactivity pathways.

Thermal and photochemical reactivities of iron nitrosyls also depend on the nature of the co-ligands. The correlation between the structure and reactivity of sulfur-containing iron nitrosyls is a tool for elucidation of the chemical and physiological behaviour of natural and artificial NO-donors, carriers and acceptor sites and may help to design novel, safe and more efficient drugs.

Acknowledgement

K.S. thanks the Rector of the Jagiellonian University for the fellowship.

References

[1] D.R. Adams, M. Brochwicz-Lewinski, A.R. Butler, Progr. Chem. Org. Nat. Prod. 76 (1999) 1.
[2] R.F. Furchgott, Angew. Chem. Int. Ed. 38 (1999) 1871.
[3] L.J. Ignarro, Angew. Chem. Int. Ed. 38 (1999) 1883.
[4] F. Murad, Angew. Chem. Int. Ed. 38 (1999) 1875.
[5] L.J. Hofseth, S.P. Hussain, G.N. Wogan, C.C. Harris, Free Radical Biol. Med. 34 (2003) 955.
[6] I.M. Wasser, S. de Vries, P. Moenne-Loccoz, I. Schroeder, K.D. Karlin, Chem. Rev. 102 (2002) 1201.
[7] G.M. Rosen, P. Tsai, S. Pou, Chem. Rev. 102 (2002) 1191.
[8] P.C. Ford, I. Lorkovic, Chem. Rev. 102 (2002) 993.
[9] A.R. Butler, I.L. Megson, Chem. Rev. 102 (2002) 1155.
[10] T.W. Hayton, P. Legzdins, W.B. Sharp, Chem. Rev. 102 (2002) 935.
[11] M. Feelisch, J.S. Stamler (Eds.), Methods in Nitric Oxide Research, John Wiley & Sons, Chicester, 1996.
[12] Z. Stasicka, E. Wasielewska, Coord. Chem. Rev. 159 (1997) 271.
[13] G. Stochel, M. Pawelec, Z. Stasicka, Wiad. Chem. 51 (1997) 163.
[14] K. Szaciłowski, Z. Stasicka, Coord. Chem. Rev. 229 (2002) 17.
[15] K. Szaciłowski, Chem. Eur. J. 10 (2004) 2520.
[16] K. Szaciłowski, Z. Stasicka, Progr. React. Kin. Mech. 26 (2001) 1.
[17] L. Laverman, A. Wanat, J. Oszajca, G. Stochel, P.C. Ford, R. van Eldik, J. Am. Chem. Soc. 123 (2001) 285.
[18] A. Wanat, J. Gdula-Argasińska, D. Rutkowska-Żbik, M. Witko, G. Stochel, R. van Eldik, J. Biol. Inorg. Chem. 7 (2002) 165.
[19] A. Wanat, M. Wolak, M. Orzeł, R. Brindell, G. van Eldik, Stochel, Coord. Chem. Rev. 229 (2002) 37.
[20] M. Wolak, A. Zahl, T. Schneppensieper, G. Stochel, R. van Eldik, J. Am. Chem. Soc. 123 (2001) 9780.
[21] E. Wasielewska, Z. Stasicka, J. Inf. Rec. Mater. 17 (1989) 441.
[22] J. Oszajca, G. Stochel, E. Wasielewska, Z. Stasicka, R.J. Gryglewski, A. Jakubowski, K. Cieślik, J. Inorg. Biochem. 69 (1998) 121.
[23] K. Szaciłowski, G. Stochel, Z. Stasicka, H. Kisch, New. J. Chem. 21 (1997) 893.
[24] K. Szaciłowski, A. Wanat, A. Barbieri, E. Wasielewska, M. Witko, G. Stochel, Z. Stasicka, New. J. Chem. 26 (2002) 1495.
[25] G.A. Lawrence, M. Maeder, Y.-M. Neuhold, K. Szaciłowski, A. Barbieri, Z. Stasicka, J. Chem. Soc. Dalton Trans. (2002) 3649.
[26] T. Schneppensieper, A. Wanat, G. Stochel, S. Goldstein, D. Meyerstein, R. van Eldik, Eur. J. Inorg. Chem. (2001) 2317.
[27] T. Schneppensieper, A. Wanat, G. Stochel, R. van Eldik, Inorg. Chem. 41 (2002) 2565.
[28] A. Wanat, T. Schneppensieper, A. Karocki, G. Stochel, R. van Eldik, J. Chem. Soc. Dalton Trans. (2002) 941.
[29] A. Wanat, T. Schneppensieper, G. Stochel, R. van Eldik, E. Bill, K. Wieghardt, Inorg. Chem. 41 (2002) 4.
[30] M. Wolak, R. van Eldik, Coord. Chem. Rev. 230 (2002) 263.
[31] G. Stochel, R. van Eldik, E. Hejmo, Z. Stasicka, Inorg. Chem. 27 (1988) 2767.
[32] G. Stopa, Z. Stasicka, Polyhedron 3 (1984) 247.
[33] G. Stochel, Z. Stasicka, Polyhedron 4 (1985) 481.
[34] G. Stochel, Coord. Chem. Rev. 114 (1992) 269.
[35] G. Stochel, Zesz. Nauk. UJ (Chemia) 29 (1985) 97.
[36] T. Senkowski, Zesz. Nauk. UJ (Chemia) 13 (1968) 7.
[37] T. Senkowski, Rocz. Chem. 42 (1968) 2007.

[38] T. Jarzynowski, T. Senkowski, Z. Stasicka, Rocz. Chem. 51 (1977) 2299.
[39] E. Hejmo, E. Porcel-Ortega, T. Senkowski, Z. Stasicka, Bull. Pol. Acad. Sci. Chem. 36 (1988) 351.
[40] G. Stochel, R. van Eldik, Inorg. Chim. Acta 155 (1989) 95.
[41] G. Stochel, G. Stopa, Z. Stasicka, Bull. Pol. Acad. Sci. Chem. 42 (1994) 473.
[42] Z. Sojka, G. Stopa, J. Chem. Educ. 70 (1993) 675.
[43] T. Senkowski, E. Hejmo, Ann. Soc. Chim. Pol. 50 (1976) 1483.
[44] J. Mikulski, T. Senkowski, I. Stroński, Kernenergie 6 (1963) 294.
[45] A. Wanat, R. van Eldik, G. Stochel, J. Chem. Soc. Dalton Trans. (1998) 2497.
[46] M. Wolak, G. Stochel, R. van Eldik, Inorg. Chem. 39 (2000) 2018.
[47] M. Wolak, G. Stochel, R. van Eldik, J. Am. Chem. Soc. 125 (2003) 1334.
[48] A. Franke, C. Jung, G. Stochel, R. van Eldik, J. Am. Chem. Soc. 126 (2004) 4181.
[49] K. Szaciłowski, Z. Stasicka, Ann. Pol. Chem. Soc. 2 (2003) 435.
[50] K. Szaciłowski, Wiad. Chem. 58 (2004) 11.
[51] G. Stopa, Z. Stasicka, D. Rehorek, Pol. J. Chem. 65 (1991) 649.
[52] A. Jańczyk, A. Wolnicka-Glubisz, A. Chmura, M. Elas, Z. Matuszak, G. Stochel, K. Urbańska, Nitric Oxide 10 (2004) 42.
[53] G. Stochel, Z. Stasicka, Polyhedron 4 (1985) 1887.
[54] G. Stochel, A. Wanat, E. Kuliś, Z. Stasicka, Coord. Chem. Rev. 171 (1998) 203.
[55] K. Szaciłowski, W. Macyk, G. Stochel, S. Sostero, O. Traverso, Z. Stasicka, Coord. Chem. Rev. 208 (2000) 277.
[56] K. Szaciłowski, J. Oszajca, A. Barbieri, A. Karocki, Z. Sojka, S. Sostero, R. Boaretto, Z. Stasicka, J. Photochem. Photobiol. A Chem. 143 (2001) 99.
[57] K. Szaciłowski, J. Oszajca, G. Stochel, Z. Stasicka, J. Chem. Soc. Dalton Trans. (1999) 2353.
[58] G. Stochel, R. van Eldik, Z. Stasicka, Inorg. Chem. 25 (1986) 3663.
[59] G. Stochel, A. Drzewiecka, E. Kuliś, M. Palarczyk, M. Pawelec, A. Wanat, M. Wolak, in: M. Melnik, A. Sirota (Eds.), Challenges for Coordination Chemistry in the New Century, Slovak Technical University Press, Bratislava, 2001.
[60] T. Jarzynowski, T. Senkowski, Z. Stasicka, Pol. J. Chem. 55 (1981) 3.
[61] Z. Stasicka, T. Senkowski, in: L. Lang (Ed.), Absorption Spectra in the Ultraviolet and Visible Region, Budapest, 1962.
[62] E. Wasielewska, M. Witko, G. Stochel, Z. Stasicka, Chem. Eur. J. 3 (1997) 609.
[63] M. Pawelec, A. Siedlecki, A. Bassara, O. Wenhrynowicz, A. Dembińska-Kieć, Rev. Iberoamer. Thromb. Haemostasia 7 (1994) 79.
[64] G. Stochel, E. Ilkowska, M. Pawelec, A. Wanat, M. Wolak, Acta Chim. Hung. Models Chem. 135 (1998) 847.
[65] A. Chmura, K. Szaciłowski, Z. Stasicka, in preparation.
[66] M. Jaworska, Z. Stasicka, J. Organomet. Chem. 689 (2004) 1702.
[67] A. Gołębiewski, E. Wasielewska, J. Mol. Struct. 67 (1980) 183.
[68] A. Gołębiewski, E. Rzeszowska, Acta Phys. Pol. 45 (1974) 563.
[69] E. Wasielewska, Inorg. Chim. Acta 113 (1986) 115.
[70] B. Gaston, Biochem. Biophys. Acta 1411 (1999) 323.
[71] C.E. Cooper, Biochem. Biophys. Acta 1411 (1999) 290.
[72] L.J. Ignarro, J. Physiol. Pharm. 53 (2002) 503.
[73] G.C. Brown, Biochem. Biophys. Acta 1411 (1999) 351.
[74] D.A. Wink, J.B. Mitchell, Free Radical Biol. Med. 25 (1998) 434.
[75] R.J. Nelson, L.J. Kriegsfield, V.L. Davson, T.M. Davson, Front. Neuroendocrynol. 18 (1997) 463.
[76] A.L. Burnett, Urology 45 (1995) 1071.
[77] L. Trabace, K.M. Kendrick, J. Neurochem. 75 (2000) 1664.
[78] V.D. Dixit, N. Parvizi, Anim. Reprod. Sci. 65 (2001) 1.
[79] M.J. Millan, Progr. Neurobiol. 66 (2002) 355.
[80] M. Hoshino, L. Laverman, P.C. Ford, Coord. Chem. Rev. 187 (1999) 75.
[81] M. Milani, A. Pesce, M. Nardini, H. Ouellet, Y. Ouellet, S. Dewilde, A. Bocedi, P. Ascenzi, M. Guertin, L. Moens, J.M. Friedman, J.B. Wittenberg, M. Bolognesi, J. Inorg. Biochem. 99 (2005) 97.
[82] B. Pal, T. Kitagawa, J. Inorg. Biochem. 99 (2005) 267.
[83] I. Endo, M. Odaka, M. Yohda, Trends Biotechnol. 17 (1999) 244.
[84] T. Noguchi, M. Noriji, K. Takei, M. Odaka, N. Kamiya, Biochemistry 42 (2003) 11642.
[85] M.-A. Gilles-Gonzalez, G. Gonzalez, J. Inorg. Biochem. 99 (2005) 1.
[86] B. Alexander, Nutrition 14 (1998) 376.
[87] K. Xie, S. Huang, Free Radical Biol. Med. 34 (2003) 969.
[88] J.L. Bourassa, W. DeGraff, S. Kudo, D. Wink, J. Mitchell, P.C. Ford, J. Am. Chem. Soc. 119 (1997) 2853.
[89] J.W. Denninger, M.A. Marletta, Biochem. Biophys. Acta 1411 (1999) 334.
[90] I.S. Severina, O.G. Bussygina, N.V. Pyatakova, I.V. Malenkova, A.F. Vanin, Nitric Oxide 8 (2003) 155.
[91] A.R. Butler, F.W. Flitney, D.L.H. Williams, Trends Pharmacol. Sci. 16 (1995) 18.
[92] D.S. Bohle, Curr. Opin. Chem. Biol. 2 (1998) 194.
[93] M. Hughes, Biochem. Biophys. Acta 1411 (1999) 263.
[94] M. Kelm, Biochem. Biophys. Acta 1411 (1999) 272.
[95] R.P. Patel, J. McAndrew, H. Sellak, C.R. White, H. Jo, B.A. Freeman, V.M. Darley-Usmar, Biochem. Biophys. Acta 1411 (1999) 385.
[96] J.S. Stamler, D.J. Singel, J. Loscalzo, Science 258 (1992) 1898.
[97] P.J. Farmer, F. Sulc, J. Inorg. Biochem. 99 (2005) 166.
[98] S. Goldstein, G. Czapski, J. Am. Chem. Soc. 117 (1995) 12078.
[99] M.E. Murphy, H. Seis, Proc. Natl. Acad. Sci. U.S.A. 88 (1991) 10860.
[100] V. Shafirovich, S.V. Lymar, Proc. Natl. Acad. Sci. U.S.A. 99 (2002) 7340.
[101] S.I. Liochev, I. Fridovich, Arch. Biochem. Biophys. 402 (2002) 166.
[102] M.A. Sharpe, C.E. Cooper, Biochem. J. 332 (1988) 9.
[103] J.J. Poderoso, M.C. Carreras, F. Shopfer, C.L. Lisdero, N.A. Riobo, C. Giulivi, A.D. Boveris, A. Boveris, E. Cadenas, Free Radical Biol. Med. 26 (1999) 925.
[104] S. Adak, Q. Wang, D.J. Stuehr, J. Biol. Chem. 275 (2000) 33554.
[105] S.I. Liochev, I. Fridovich, Free Radical Biol. Med. 34 (2003) 1399.
[106] K.M. Miranda, A.S. Dutton, L.A. Ridnour, C.A. Foreman, E. Ford, N. Paolocci, T. Katori, C.G. Tocchetti, D. Mancardi, D.D. Thomas, M.G. Espey, K.N. Houk, J.M. Fukuto, D.A. Wink, J. Am. Chem. Soc. 127 (2004) 722.
[107] P.S.-Y. Wong, J. Hyun, J.M. Fukuto, F.N. Shirota, E.G. DeMaster, D.W. Shoeman, H.T. Nagasawa, Biochemistry 37 (1998) 18129.
[108] M. Feelisch, Proc. Natl. Acad. Sci. U.S.A. 100 (2003) 4978.
[109] K.D. Kröncke, K. Fehsel, V. Kolb-Bachofen, Nitric Oxide 1 (1997) 107.
[110] C. Szabó, Toxicology Lett. 140–141 (2003) 105.
[111] J.P. Crow, Free Radical Biol. Med. 28 (2000) 1487.
[112] C. Jacob, G.I. Giles, M.N. Giles, H. Sies, Angew. Chem. Int. Ed. 42 (2003) 4742.
[113] A. Pompella, G. Bahegyi, M. Wellman-Rousseu (Eds.), Thiol Metabolism and Redox Regulation of Cellular Functions, IOS Press, Amsterdam, 2002.
[114] C. Gilter, A. Danon (Eds.), Cellular Implications of Redox Signalling, World Scientific, Singapore, 2003.
[115] Y.M. Torchinsky, Sulfur in Proteins, Pergamon Press, Oxford, 1981.
[116] P.C. Joselyn, Biochemistry of the SH Group, Academic Press, London, 1971.
[117] R.C. Fahey, Adv. Exp. Med. Biol. 86A (1977) 1.
[118] T.P. Akerboom, M. Bilzer, H. Sies, J. Biol. Chem. 257 (1982) 4248.
[119] B. Kalyanaraman, Biochem. Soc. Symp. 61 (1995) 55.
[120] P. Girard, P. Potier, FEBS Lett. 320 (1993) 7.
[121] M.G. Bonini, O. Augusto, J. Biol. Chem. 276 (2001) 9749.

[122] H. Karoui, N. Hogg, C. Frejaville, P. Tordo, B. Kalyanaraman, J. Biol. Chem. 271 (1996) 600.
[123] M. Jonsson, H.-B. Kraatz, J. Chem. Soc. Perkin Trans. 2 (1997) 2673.
[124] R. Zhao, J. Lind, G. Merényi, T.E. Eriksen, J. Chem. Soc. Perkin Trans. 2 (1997) 569.
[125] A. Del Corso, P.G. Vilardo, M. Cappiello, I. Cecconi, M. Dal Monte, D. Barsacchi, U. Mura, Arch. Biochem. Biophys. 397 (2002) 392.
[126] C. El Hanine Lmoumene, D. Conte, J.-P. Jacquot, C. Houee-Levin, Res. Chem. Intermed. 25 (1999) 313.
[127] S.P. Mezyk, J. Phys. Chem. 100 (1996) 8861.
[128] Y. Gauduel, J.L. Marignier, J. Belloni, H. Gelabert, J. Phys. Chem. A 101 (1997) 8979.
[129] S. Carles, F. Lecomte, J.P. Schermann, C. Desfrancois, S. Xu, J.M. Nilles, K.H. Bowen, J. Berges, C. Houee-Levin, J. Phys. Chem. A 105 (2001) 5622.
[130] S.P. Mezyk, Chem. Phys. Lett. 235 (1995) 89.
[131] S.P. Mezyk, D.A. Armstrong, J. Chem. Soc. Perkin Trans. 2 (1999) 1411.
[132] S. Raina, D. Missiakas, Annu. Rev. Microbiol. 51 (1997) 179.
[133] R.J.P. Williams, J.J.R. Frausto da Silva, Coord. Chem. Rev. 200–202 (2000) 247.
[134] R.H. Holm, P. Kennepohl, E.I. Solomon, Chem. Rev. 96 (1996) 2239.
[135] www.webelements.com.
[136] A. Messesrschmidt, R. Huber, T. Poulos, K. Wieghart (Eds.), Handbook of Metalloproteins, John Wiley & Sons, Ltd., NY, 2001.
[137] PROMISE database available at http://metallo.scripps.edu/PROMISE/MAIN.html, 1998.
[138] J.M. Castagnetto, S.W. Hennessy, V.A. Roberts, E.D. Getzoff, J.A. Tainer, M.E. Pique, Nucleic Acid Res. 30 (2002) 379.
[139] P.J. Stephens, D.R. Jolie, A. Warshel, Chem. Rev. 96 (1996) 2491.
[140] A.W. Bott, Curr. Sep. 18 (1999) 4754.
[141] D.L. Harris, Curr. Opin. Chem. Biol. 5 (2001) 724.
[142] H. Fujii, Coord. Chem. Rev. 226 (2002) 51.
[143] J.E. Cornah, M.J. Terry, A.G. Smith, Trends Plant Sci. 8 (2003) 224.
[144] L.R. Milgrom, The Colours of Life, O.U. Press, Oxford, 1997.
[145] F. Torrens, Molecules 9 (2004) 632.
[146] R. Jain, M.K. Chan, J. Biol. Inorg. Chem. 8 (2003) 1.
[147] T. Brittain, J. Inorg. Biochem. 99 (2005) 120.
[148] J.A. Cowan, Inorganic Biochemistry: An Introduction, VCH Publishers, NY, 1993.
[149] T. Hankeln, B. Ebner, C. Fuchs, F. Gerlach, M. Haberkamp, T.L. Laufs, A. Roesner, M. Schmidt, B. Weich, S. Wystub, S. Saaler-Reinhardt, S. Reuss, M. Bolognesi, D. De Sanctis, M.C. Marden, L. Kiger, L. Moens, S. Dewilde, E. Nevo, A. Avivi, R.E. Weber, A. Fago, T. Burmester, J. Inorg. Biochem. 99 (2005) 110.
[150] R.E. Weber, A. Fago, Resp. Physiol. Neurobiol. 144 (2004) 141.
[151] W. Kaim, B. Schwederski, Bioinorganic Chemistry: Inorganic Elements in the Chemistry of Life, Wiley, Chichester, 1991.
[152] R. Bantleon, J. Altenbuchner, K.H. van Pee, J. Bacteriol. 176 (1994) 2339.
[153] L.A. Andersson, L.A. Dawson, Struct. Bond. 64 (1991) 1.
[154] S. Ferguson-Miller, G.T. Babcock, Chem. Rev. 96 (1996) 2889.
[155] G.R. Moore, G.W. Pettigrew, Cytochromes *c*. Evolutionary, Structural and Physicochemical Aspects, S. Varlag, Heidelberg, 1990.
[156] M.C. Silvestrini, S. Falcinelli, I. Ciabatti, F. Cutruzzola, M. Brunori, Biochemie 76 (1994) 641.
[157] T. Brittain, R. Blackmore, C. Greenwood, A.J. Thomson, Eur. J. Biochem. 209 (1992) 793.
[158] R.C. Prince, G.N. George, Nat. Struct. Biol. 4 (1997) 247.
[159] R.H. Holm, Pure Appl. Chem. 70 (1998) 931.
[160] H. Beinert, J. Biol. Inorg. Chem. (2000) 2.
[161] H. Beinert, R.H. Holm, E. Münck, Science 277 (1997) 653.
[162] M.E. Stroupe, E.D. Getzoff, in: A. Messesrschmidt, R. Huber, T. Poulos, K. Wieghart (Eds.), Handbook of Metalloproteins, John Wiley & Sons, Ltd., NY, 2001.
[163] N. Arulsalmy, S.D. Bohle, J.A. Butt, G.J. Irvine, P.A. Jordan, E. Sagan, J. Am. Chem. Soc. 121 (1999) 7115.
[164] L. Field, R.V. Dilts, R. Ravichandran, P.G. Lenhert, G.E. Carnahan, J. Chem. Soc. Chem. Commun. (1978) 249.
[165] G.E. Carnahan, P.G. Lenhert, R. Ravichandran, Acta Crystallogr. B 33 (1978) 3332.
[166] P.V. Bharatam, P. Amita, Senthilkumar, Tetrahedron 60 (2004) 4801.
[167] N. Bainbridge, A.R. Butler, C.H. Görbitz, J. Chem. Soc. Perkin Trans. 2 (1997) 351.
[168] A. Martinez-Ruiz, S. Lamas, Cardiovasc. Res. 62 (2004) 43.
[169] N. Hogg, R.J. Singh, B. Kalyanamaran, FEBS Lett. 382 (1996) 223.
[170] J.P. Eiserich, R.P. Patel, V.B. O'Donnell, Mol. Aspects Med. 19 (1998) 221.
[171] K.N. Houk, B.N. Hietbrink, M.D. Bartberger, P.R. McCarren, B.Y. Choi, R.D. Voyksner, J.S. Stamler, E.J. Toone, J. Am. Chem. Soc. 125 (2003) 6972.
[172] L.L. Perissilotti, A.G. Turjanski, D.A. Estrin, F. Doctorovich, J. Am. Chem. Soc. 127 (2005) 486.
[173] J.S. Stamler, E.J. Toone, Curr. Opin. Chem. Biol. 6 (2002) 779.
[174] R.J. Singh, J.S. Wishnok, M. Keshive, W.M. Deen, S.R. Tannenbaum, Proc. Natl. Acad. Sci. U.S.A. 93 (1996) 14428.
[175] S. Bian, J.A. Cowan, Coord. Chem. Rev. 190–192 (1999) 1049.
[176] D.H. Flint, R.M. Allen, Chem. Rev. 96 (1996) 2315.
[177] H. Beinert, M.C. Kennedy, C.D. Stout, Chem. Rev. 96 (1996) 2335.
[178] M.J. Mahe, Z. Xiao, M.C.J. Wilce, J.M. Guss, A.G. Wedd, Acta Crystallogr. D 55 (1999) 962.
[179] C. Bida, A. Coda, A. Aliverti, G. Zanetti, A. Mattevi, Acta Crystallogr. D 54 (1998) 1353.
[180] L.M. Hunsicker-Wang, A. Heine, Y. Chen, E.P. Luna, T. Todaro, Y.M. Zhang, P.A. Williams, D.E. McRee, J. Hirst, Biochemistry 42 (2003) 7303.
[181] S. Aono, D. Bentrop, I. Bertini, A. Donaire, C. Luchinat, Biochemistry 37 (1998) 9812.
[182] P. Strop, P.M. Tatahara, H.-J. Chiu, H.C. Angove, Biochemistry 40 (2001) 651.
[183] B. Schmid, M.W. Ribbe, O. Einsle, M. Yoshida, L.M. Thomas, D.R. Dean, D.C. Rees, B.K. Burges, Science 296 (2002) 352.
[184] J. Kim, D.C. Rees, Science 257 (1992) 1677.
[185] B.R. Crane, L.M. Siegel, E.D. Getzoff, Biochemistry 36 (1997) 12120.
[186] D.C. Rees, J.B. Howard, Science 300 (2003) 929.
[187] M.K. Johnson, Curr. Opin. Chem. Biol. 2 (1998) 173.
[188] C. Huber, G. Wächtenhäuser, Science 281 (1998) 670.
[189] R. Hoffmann, M.M.L. Chen, D.L. Thorn, Inorg. Chem. 16 (1977) 503.
[190] M.W. Degroot, J.F. Corrigan, in: J.A. McCleverty, T.J. Meyer (Eds.), Comprehensive Coordination Chemistry II, Elsevier, Amsterdam, 2003.
[191] Y. Niu, H. Zheng, H. Hou, X. Xin, Coord. Chem. Rev. 248 (2004) 169.
[192] M.N. Sokolov, V.P. Fedin, Coord. Chem. Rev. 248 (2004) 925.
[193] H. Ogino, S. Inomata, H. Tobita, Chem. Rev. 98 (1998) 2093.
[194] G. Henkel, B. Krebs, Chem. Rev. 104 (2004) 801.
[195] I.V. Kalinina, V.P. Fedin, Russ. J. Coord. Chem. 29 (2003) 597.
[196] P.F. Kelly, Annu. Rep. Prog. Chem. Sect. A 95 (1999) 67.
[197] S. Dey, V.K. Jain, Platinum Metals Rev. 48 (1) (2004) 16.
[198] T. Shibahara, Coord. Chem. Rev. 123 (1993) 73.
[199] R.H. Holm, in: J.A. McCleverty, T.J. Meyer (Eds.), Comprehensive Coordination Chemistry II, Elsevier, Amsterdam, 2003.
[200] P.V. Rao, R.H. Holm, Chem. Rev. 104 (2004) 527.
[201] J.B. Broderick, in: J.A. McCleverty, T.J. Meyer (Eds.), Comprehensive Coordination Chemistry II, Elsevier, Amsterdam, 2003.

[202] R.H. Holm, Adv. Inorg. Chem. 38 (1992) 1.
[203] E. Nordlander, A.M. Whalen, Coord. Chem. Rev. 142 (1995) 43.
[204] M.D. Ward, Coord. Chem. Rev. 115 (1992) 1.
[205] S.M. Nelson, in: G. Wilkinson, R.D. Gillard, J.A. McClevery (Eds.), Comprehensive Coordination Chemistry, Pergamon Press, Oxford, 1987.
[206] W. Bronger, Z. Anorg. Allg. Chem. 359 (1968) 225.
[207] J.F. You, B.S. Snyder, G.C. Papaefthymiou, R.H. Holm, J. Am. Chem. Soc. 112 (1990) 1067.
[208] G.R. Long, R.H. Holm, Inorg. Chim. Acta 229 (1995) 229.
[209] C. Goh, B.M. Segal, J. Huahg, G.R. Long, R.H. Holm, J. Am. Chem. Soc. 118 (1996) 11844.
[210] U. Geiser, J.M. Williams, Acta Crystallogr. C 54 (1998) 292.
[211] L.L. Martin, G.D. Fallon, B. Wu, Acta Crystallogr. E 60 (2004) i37.
[212] C.T.-W. Chu, F.Y.-K. Lo, L.F. Dahl, J. Am. Chem. Soc. 104 (1982) 3409.
[213] A.R. Butler, C. Glidewell, M.H. Li, Adv. Inorg. Chem. 32 (1988) 335.
[214] M.-L. Tsai, C.-C. Chen, I.-J. Hsu, S.-C. Ke, C.-H. Hsieh, K.-A. Chiang, G.-H. Lee, Y. Wang, J.-M. Chen, J.F. Lee, W.-F. Liaw, Inorg. Chem. 43 (2004) 5159.
[215] E.A. Pasek, D.K. Straub, Inorg. Chem. 11 (1971) 259.
[216] J.A. Cras, J. Willemse, in: G. Wilkinson, R.D. Gillard, J.A. McClevery (Eds.), Comprehensive Coordination Chemistry, Pergamon Press, Oxford, 1987.
[217] B. Meunier, S.P. de Visser, S. Shaik, Chem. Rev. 104 (2004) 3947.
[218] P. Rydberg, E. Sigfridsson, U. Ryde, J. Biol. Inorg. Chem. 9 (2004) 203.
[219] F. Tani, M. Matsu-ura, S. Nakayama, Y. Naruta, Coord. Chem. Rev. 226 (2002) 219.
[220] J.L.R. Anderson, S.K. Chapman, Dalton Trans. (2005) 13.
[221] P. Hlavic, Eur. J. Biochem. 271 (2004) 4335.
[222] D. Mansuy, Pure Appl. Chem. 66 (1994) 737.
[223] F. Ogliaro, S.P. de Visser, S. Shaik, J. Inorg. Biochem. 91 (2002) 554.
[224] J.H. Enemark, R.D. Feltham, Coord. Chem. Rev. 13 (1974) 339.
[225] P.C. Ford, L. Laverman, I. Lorkovic, Adv. Inorg. Chem. 54 (2004) 203.
[226] J.R. Stone, M.A. Marletta, Biochemistry 33 (1994) 5636.
[227] V. Vasta, J. Beavo, Cell Transm. 20 (2004) 1.
[228] S.R. Piersma, N. Nojiri, M. Tsujimura, T. Noguchi, M. Odaka, M. Yohda, Y. Inoue, J. Inorg. Biochem. 80 (2000) 283.
[229] I. Endo, M. Nojiri, M. Tsujimura, M. Nakasako, S. Nagashima, M. Yohda, M. Odaka, J. Inorg. Biochem. 83 (2001) 247.
[230] M.G. Sauaia, F. de Souza Oliveira, A.C. Tedesco, R. Santana da Silva, Inorg. Chim. Acta 355 (2003) 191.
[231] S.N. Greene, N.G.J. Richards, Inorg. Chem. 43 (2004) 7030.
[232] D. Giustrani, A. Milzani, R. Colombo, I. Dalle-Donne, R. Rossi, Trends Pharm. Sci. 25 (2004) 311.
[233] A.J. Gow, J.S. Stamler, Nature 391 (1998) 169173.
[234] Y. Henry, A. Gussani, Cell. Mol. Life Sci. 55 (1999) 1003.
[235] A.J. Hobbs, M.T. Gladwin, R. Patel, D.L.H. Williams, A.R. Butler, Trends Pharm. Sci. 23 (2002) 406.
[236] H. Kosaka, Biochim. Biophys. Acta 1411 (1999) 370.
[237] Y. Zhang, N. Hogg, Free Radical Biol. Med. 36 (2004) 947.
[238] E.J. Frehm, G. Bonaventura, A.J. Gow, Free Radical Biol. Med. 37 (2004) 442.
[239] J.F. Andersen, A. Weichsel, C.A. Balfour, D.E. Champagne, W.R. Montfort, Structure 6 (1998) 1315.
[240] J.F. Andersen, W.R. Montfort, J. Biol. Chem. 275 (2000) 30396.
[241] P. Ascenzi, M. Nardini, M. Bolognesi, W.R. Montfort, Biochem. Mol. Biol. Educ. 30 (2002) 68.
[242] D.E. Champagne, R.H. Nussenzweig, J.M.C. Ribeiro, J. Biol. Chem. 270 (1995) 8691.
[243] W.R. Montfort, A. Weichsel, J.F. Andersen, Biochim. Biophys. Acta 1482 (2000) 110.
[244] T. Gérczei, Á. Fazekas, G.M. Keserű, J. Mol. Struct. (Theochem.) 503 (2000) 51.
[245] P.C. Ford, J. Bourassa, K. Miranda, B. Lee, I. Lorkovic, S. Boggs, S. Kudo, L. Laverman, Coord. Chem. Rev. 171 (1998) 185.
[246] P.C. Ford, L.E. Laverman, I.M. Lorkovic, Adv. Inorg. Chem. 54 (2003) 203.
[247] J.A. McCleverty, Chem. Rev. 104 (2004) 403.
[248] M.D. Lim, I. Lorkovic, P.C. Ford, J. Inorg. Biochem. 99 (2005) 151.
[249] W. Macyk, A. Franke, G. Stochel, Coord. Chem. Rev. (2005) in press.
[250] L. Cambi, Atti. Acad. Nazl. Linzei. 24 (1915) 434.
[251] P.T. Manoharan, H.B. Gray, J. Am. Chem. Soc. 87 (1965) 3340.
[252] P. Boulet, M. Buchs, H. Chermette, C. Daul, E. Furet, F. Gilardoni, F. Rogemond, C.W. Schlapfer, J. Weber, J. Phys. Chem. A 105 (2001) 8999.
[253] M. Buchs, C.A. Daul, P.T. Manoharan, C.W. Schlaepfer, Int. J. Quant. Chem. 91 (2003) 418.
[254] M.C.G. Lebrero, D.A. Scherlis, G.L. Estiu, J.A. Olabe, D.A. Estrin, Inorg. Chem. 40 (2001) 4127.
[255] Y. Marcus, Ion Solvation, Wiley, NY, 1985.
[256] D. Wendehenne, A. Pugin, D.F. Klessig, J. Duner, Trends Plant Sci. 6 (2001) 177.
[257] P. Wojtaszek, Phytochemistry 54 (2000) 1.
[258] L.A. del Rio, F.J. Corpas, J.B. Barroso, Phytochemistry 65 (2004) 783.
[259] J.T. Groves, C.C.-Y. Wang, Curr. Opin. Chem. Biol. 4 (2000) 687.
[260] M.-H. Zhou, C. Shi, R.A. Cohen, J. Clin. Invest. 109 (2002) 817.
[261] P.J. Andrew, B. Mayer, Cardiovasc. Res. 43 (1999) 521.
[262] A. Schwentker, T.R. Billiar, World Surg. J. 26 (2002) 772.
[263] V. Ullrich, Arch. Biochem. Biophys. 409 (2003) 45.
[264] D.J. Stuehr, Biochem. Biophys. Acta 1411 (1999) 217.
[265] I. Sagami, Y. Sato, T. Noguchi, M. Miyajima, E. Rozhkova, S. Daff, T. Shimizu, Coord. Chem. Rev. 226 (2002) 179.
[266] M.A. Marletta, A.R. Hurshman, K.M. Rusche, Curr. Opin. Chem. Biol. 2 (1998) 656.
[267] D.L. Rousseau, D. Li, M. Couture, S.R. Yeh, J. Inorg. Biochem. 99 (2005) 306.
[268] D.L. Harris, Int. J. Quant. Chem. 88 (2001) 183.
[269] S. Yoshioka, S. Takahashi, H. Hori, K. Ishimori, I. Morishima, Eur. J. Biochem. 268 (2001) 252.
[270] M.C. Feiters, A.E. Rowan, R.J.M. Nolte, Chem. Soc. Rev. 29 (2000) 375.
[271] M.T. Green, J. Am. Chem. Soc. 121 (1999) 7939.
[272] T. Ohta, K. Matsuura, K. Yoshizawa, I. Morishima, J. Inorg. Biochem. 82 (2000) 141.
[273] A. Müller, E. Diemann, in: G. Wilkinson, R.D. Gillard, J.A. McClevery (Eds.), Comprehensive Coordination Chemistry, Pergamon Press, Oxford, 1987.
[274] J.S. Stamler, L. Jia, J.P. Eu, T.J. McMahon, I.T. Demchenko, J. Bonaventura, K. Gernert, C.A. Piandosi, Science 276 (1997) 2034.
[275] M.T. Gladwin, X. Wang, C.D. Reiter, B.K. Yang, E.X. Vivas, C. Bonaventura, A.N. Schechter, J. Biol. Chem. 277 (2002) 27818.
[276] T. Gladwin, J.R. Lancaster, B.A. Freeman, A.N. Schechter, Nat. Med. 9 (2003) 496.
[277] J.H. Crawford, C.R. White, R.P. Patel, Blood 101 (2003) 4408.
[278] M.T. Gladwin, J.H. Crawford, R.P. Patel, Free Radical Biol. Med. 36 (2004) 707.
[279] S. Deem, S.S. Kim, J.-H. Min, R. Eveland, J. Moulding, S. Martyr, X. Wang, E.R. Swenson, M.T. Gladwin, Am. J. Physiol. Heart Circ. Physiol. 287 (2004) H2561.
[280] A. Daiber, H. Shoun, V. Ullrich, J. Inorg. Biochem. 99 (2005) 185.
[281] Y. Shiro, RIKEN Rev. 24 (1999) 56.
[282] S. Kuznetsova, D.B. Knaff, M. Hirasawa, B. Lagoutte, P. Setif, Biochemistry 43 (2004) 510.

[283] J.G. Valenzuela, F.A. Walker, J.M.C. Ribeiro, J. Exp. Biol. 198 (1995) 1519.
[284] F.A. Walker, J. Inorg. Biochem. 99 (2005) 216.
[285] A. Weichsel, E.M. Maes, J.F. Andersen, J.G. Valenzuela, T.K. Shokhireva, F.A. Walker, W.R. Montfort, Proc. Natl. Acad. Sci. U.S.A. 102 (2005) 594.
[286] S. Nagashima, M. Nakasako, N. Dohmae, M. Tsujimura, K. Takio, M. Odaka, M. Yohda, N. Kamiya, I. Endo, Nat. Struct. Biol. 5 (1998) 347.
[287] H. Yamada, M. Kobayashi, Biosci. Biotechnol. Biochem. 60 (1996) 1391.
[288] J.M. Wyatt, C.J. Knowles, Biodegradation 6 (1995) 93.
[289] I. Endo, M. Odaka, J. Mol. Catal. B Enzym. 10 (2000) 81.
[290] S.N. Greene, C.H. Chang, N.G.J. Richards, Chem. Commun. (2002) 2386.
[291] M. Odaka, K. Fujii, M. Hoshino, T. Noguchi, M. Tsujimura, S. Nagashima, M. Yohda, T. Nagamune, Y. Inoue, I. Endo, J. Am. Chem. Soc. 119 (1997) 3785.
[292] D. Schweitzer, J.J. Ellison, S.C. Shoner, S. Lovell, J.A. Kovacs, J. Am. Chem. Soc. 120 (1998) 10996.
[293] J.C. Noveron, M.M. Olmstead, P.K. Maacharak, J. Am. Chem. Soc. 123 (2001) 3247.
[294] J. Shearer, H.L. Jackson, D. Schweitzer, D.K. Rittenberg, M.T. Leavy, W. Kaminsky, R.C. Scarrow, J.A. Kovacs, J. Am. Chem. Soc. 124 (2002) 11417.
[295] C.-M. Lee, C.-H. Hsieh, A. Dutta, G.-H. Lee, W.-F. Liaw, J. Am. Chem. Soc. 125 (2003) 11492.
[296] C.-Y. Chiang, M.L. Miller, J.H. Reibenspies, M.Y. Darensbourg, J. Am. Chem. Soc. 126 (2004) 10867.
[297] J.A. Kovacs, Chem. Rev. 104 (2004) 825.
[298] F.Z. Roussin, Ann. Chim. Phys. 52 (1858) 285.
[299] O. Pavel, Ber. Dtsch. Chem. Ges. 15 (1882) 2600.
[300] K.A. Hoffmann, O.F. Wiede, Z. Anorg. Allg. Chem. 9 (1895) 295.
[301] P.G. Wang, M. Xian, X. Tang, X. Wu, Z. Wen, T. Cai, A.J. Janczuk, Chem. Rev. 102 (2002) 1091.
[302] E.K. Matthews, E.D. Seaton, M.J. Forsyth, P.P.A. Humphrey, Br. J. Pharmacol. 113 (1994) 87.
[303] F.W. Flitney, I.L. Megson, J.L.M. Thomson, G.D. Kennovin, A.R. Butler, Br. J. Pharmacol. 117 (1996) 1549.
[304] F.W. Flitney, I.L. Megson, D.E. Flitney, A.R. Butler, Br. J. Pharmacol. 107 (1992) 842.
[305] L. Noodleman, D.A. Case, Adv. Inorg. Chem. 38 (1992) 423.
[306] X.-Y. Cui, C.L. Joannou, M.N. Hughes, R. Cammack, FEMS Microbiol. Lett. 98 (1992) 67.
[307] A.B.G. Grever, A. Ruiter, Eur. Food Res. Technol. 213 (2001) 165.
[308] M.J. Scott, R.H. Holm, Angew. Chem. Int. Ed. 32 (1993) 564.
[309] C. Goh, R.H. Holm, Inorg. Chim. Acta 270 (1998) 46.
[310] C. Glidewell, J. McGinnis, Inorg. Chim. Acta 64 (1982) L171.
[311] S. Costanzo, S. Ménage, R. Parello, R.P. Bonomo, M. Fontecave, Inorg. Chim. Acta 318 (2001) 1.
[312] A.R. Butler, C. Glidewell, A.R. Hyde, J.C. Walton, Polyhedron 4 (1985) 797.
[313] N.A. Sanina, O.A. Rakova, S.M. Aldoshin, I.I. Chuev, E.G. Atovmyan, N.S. Ovanesyan, Russ. J. Coord. Chem. 27 (2001) 179.
[314] G. Johansson, W.N. Lipscomb, Acta Crystallogr. 11 (1958) 594.
[315] S. D'Addario, F. Demartin, L. Grossi, M.C. Iapalucci, F. Laschi, G. Longoni, P. Zanello, Inorg. Chem. 32 (1993) 1153.
[316] C.T.-W. Chu, R.S. Gall, L.F. Dahl, J. Am. Chem. Soc. 104 (1982) 737.
[317] L.M. Baltusis, K.D. Karlin, H.H. Rabinowitz, J.C. Dewan, S.J. Lippard, Inorg. Chem. 19 (1980) 2627.
[318] M. Boese, P.I. Mordvincev, A.F. Vanin, R. Busse, A. Mulsch, J. Biol. Chem. 270 (1995) 29244.
[319] C.L. Conrado, J.L. Bourassa, C. Egler, S. Wecksler, P.C. Ford, Inorg. Chem. 42 (2003) 2288.
[320] M. Boese, M.A. Keese, K. Becker, R. Busse, A. Mülsch, J. Biol. Chem. 35 (1997) 21767.
[321] F.C.A. Wiegant, I.Y. Malyshev, A.L. Kleschyov, E. van Faassen, A.F. Vanin, FEBS Lett. 455 (1999) 179.
[322] B. Jeżowska-Trzebiatowska, A. Jezierski, J. Mol. Struct. 19 (1973) 635.
[323] A.R. Butler, C. Glidewell, I.L. Johnson, Polyhedron 6 (1987) 1147.
[324] T.C.W. Mak, L. Book, C. Chung, M.K. Gallagher, S. Li-Cheng, D. Seyferth, Inorg. Chim. Acta 73 (1983) 159.
[325] A.M. Mazany, J.P. Flacher, M.K. Gallagher, D. Seyferth, Inorg. Chem. 22 (1983) 2593.
[326] O.A. Rakova, N.A. Sanina, S.M. Aldoshin, N.V. Goncharova, G.V. Shilov, Y.M. Shulga, N.S. Ovanesyan, Inorg. Chem. Commun. 6 (2003) 145.
[327] M. Lewin, K. Fisher, I. Dance, Chem. Commun. (2000) 947.
[328] W. Beck, R. Grenz, F. Gotzfried, E. Vilsmaier, Chem. Ber. 114 (1981) 3184.
[329] C. Glidewell, R.J. Lambert, M.E. Harman, M.B. Hursthouse, J. Chem. Soc. Dalton Trans. (1990) 2685.
[330] M. Jaworska, Z. Stasicka, New. J. Chem. 29 (2005) 1.
[331] M. Li, D. Bonnet, E. Bill, F. Neese, T. Weyermüller, K. Wieghardt, Inorg. Chem. 41 (2002) 3444.
[332] T.H. Dunning Jr., P.J. Hay, in: H.F. Schaeffer (Ed.), Methods of Electronic Structure Theory, Plenum Press, NY, 1977.
[333] S. Wecksler, A. Mikhailovsky, P.C. Ford, J. Am. Chem. Soc. 126 (2004) 13566.
[334] C.L. Conrado, S. Wecksler, C. Egler, D. Magde, P.C. Ford, Inorg. Chem. 43 (2004) 5543.
[335] J.L. Bourassa, B. Lee, S. Bernard, J. Schoonover, P.C. Ford, Inorg. Chem. 38 (1999) 2947.
[336] J.L. Bourassa, P.C. Ford, Coord. Chem. Rev. 200–202 (2000) 887.
[337] C.T.-W. Chu, L.F. Dahl, Inorg. Chem. 12 (1977) 3245.
[338] M. Jaworska, Z. Stasicka, unpublished results.